


Where do you think you're going? Accounting for ontogenetic and climate-induced movement in spatially stratified integrated population assessment models

Daniel R. Goethel^{1,2}  | Katelyn M. Bosley^{3,4} | Brian J. Langseth^{5,6} | Jonathan J. Deroba⁷ | Aaron M. Berger³ | Dana H. Hanselman² | Amy M. Schueller⁸

¹Southeast Fisheries Science Center, NMFS-NOAA, Miami, FL, USA

²Alaska Fisheries Science Center, NMFS-NOAA, Juneau, AK, USA

³Northwest Fisheries Science Center, NMFS-NOAA, Newport, OR, USA

⁴Washington Department of Fish and Wildlife, Port Townsend, WA, USA

⁵Pacific Islands Fisheries Science Center, NMFS-NOAA, Honolulu, HI, USA

⁶Northwest Fisheries Science Center, NMFS-NOAA, Seattle, WA, USA

⁷Northeast Fisheries Science Center, NMFS-NOAA, Woods Hole, MA, USA

⁸Southeast Fisheries Science Center, NMFS-NOAA, Beaufort, NC, USA

Correspondence

Daniel Goethel, Alaska Fisheries Science Center, NOAA, 17109 Point Lena Loop Road, Juneau, AK 99801, USA
Email: daniel.goethel@noaa.gov

Funding information

National Oceanic and Atmospheric Administration

Abstract

Understanding spatial population structure and biocomplexity is critical for determining a species' resilience to environmental and anthropogenic perturbations. However, integrated population models (IPMs) used to develop management advice for harvested populations have been slow to incorporate spatial dynamics. Therefore, limited research has been devoted to understanding the reliability of movement parameter estimation in spatial population models, especially for spatially dynamic marine fish populations. We implemented a spatial simulation–estimation framework that emulated a generic marine fish metapopulation to explore the impact of ontogenetic movement and climate-induced distributional shifts between two populations. The robustness of spatially stratified IPMs was explored across a range of movement parametrizations, including ignoring connectivity or estimating movement with various levels of complexity. Ignoring connectivity was detrimental to accurate estimation of population-specific biomass, while implementing spatial IPMs with intermediate levels of complexity (e.g. estimating movement in two-year and two-age blocks) performed best when no a priori information about underlying movement was available. One-way distributional shifts mimicking climate-induced poleward migrations presented the greatest estimation difficulties, but the incorporation of auxiliary information on connectivity (e.g. tag-recapture data) reduced bias. The continued development of spatially stratified modelling approaches should allow harvested resources to be better utilized without increased risk. Additionally, expanded collection and incorporation of unique spatially explicit data will enhance the robustness of IPMs in the future.

KEYWORDS

animal tracking data, connectivity, integrated population model, population structure, spatial modelling, stock assessment

1 | INTRODUCTION

Animal movement is a fundamental response to internal and external stimuli (e.g. foraging behaviour, spawning migrations or predator avoidance) that create a heterogeneous mosaic of habitat occupation across land- and seascapes (Allen & Singh, 2016; Jeltsch et al., 2013). Movement ecology research has led to breakthroughs in understanding an organism's motivation, capacity and cues for undergoing movement (Nathan et al., 2008). However, developing effective wildlife conservation strategies requires understanding the spatial ecology of the species (e.g. the spatiotemporal distribution of population productivity and abundance; Ciannelli et al., 2013). Upscaling from individual movements to population-level inferences of migration and habitat usage can create resolution issues and computational challenges (Bocedi, Pe'er, Heikkinen, Matsinos, & Travis, 2012; Jeltsch et al., 2013). Conversely, modelling population-level spatial dynamics avoids some of the parametrization issues associated with individual-based modelling frameworks and allows parameter estimation with relatively coarse data (e.g. typical harvest data; Chandler & Clark, 2014), but scaling issues may still be present when attempting to model population-level dynamics based on inferences from observations of individuals (e.g. a tagged animal; Plard, Fay, Kery, Cohas, & Schaub, 2019).

Integrated population models (IPMs) provide a unified estimation framework where population parameters can be estimated through incorporation of a variety of observed data sets and analytical submodels by utilizing a single, combined likelihood function (Maunder & Punt, 2013; Zipkin & Saunders, 2018). Spatially explicit IPMs are becoming increasingly common (e.g. Regehr, Hostetter, Wilson, Rode, & St. Martin, M., and Converse, S.J., 2018), because they can incorporate myriad data sources (e.g. count and tagging data) to help estimate population-scale movement dynamics. Additionally, spatially explicit IPMs can match the geographic scale of each data set, instead of assuming that a local scale study reflects the dynamics across the entire species distribution (Chandler & Clark, 2014). By explicitly assessing broad-scale spatiotemporal changes in population distributions, spatially explicit IPMs can better identify whether changes in observation frequency of a species are due to movement patterns (i.e., availability) or changes in abundance (Lowerre-Barbieri, Kays, Thorson, & Wikelski, 2019; Saunders et al., 2019). Incorporating movement dynamics into population models has become increasingly important as climate change continues to alter environmental conditions, often leading to poleward or, for some marine species, distributional shifts into deeper basins (Murphy, 2020; Pecl et al., 2017). Similarly, accounting for ontogenetic movement is necessary to understand habitat utilization patterns (e.g. Carruthers, Walter, McAllister, & Bryan, 2015), accurately interpret climate effects (Barbeaux & Hollowed, 2018) and implement informed conservation measures (e.g. the usefulness of marine reserves; White, 2015). Therefore, development of spatial models that can directly account for connectivity will improve understanding of the influence of ontogeny and climate change on

1. INTRODUCTION	142
2. MATERIALS AND METHODS	143
2.1 Overview	143
2.2 Operating Model	143
2.2.1 Movement Dynamics	145
2.2.2 Simulated Data	146
2.3 Integrated Population Models	146
2.4 Evaluation of Model Performance	147
2.5 Sensitivity Runs	148
3. RESULTS	148
3.1 Best-Performing IPM Parametrizations	148
3.2 Detriments of Ignoring or Oversimplifying Movement	148
3.3 Sensitivity Runs	150
4. DISCUSSION	152
5. CONCLUSIONS	157
ACKNOWLEDGEMENTS	157
DATA AVAILABILITY STATEMENT	157
REFERENCES	157

spatiotemporal dynamics and help implement more sustainable spatial harvest strategies (Karp et al., 2019; Link, Nye, & Hare, 2011).

In the marine realm, spatiotemporal dynamics are complicated by increased diffusivity and transient features, stronger scale dependence of marine processes and the larger spatial extent of many marine habitats compared to landscapes (Hidalgo, Secor, & Browman, 2016). Thus, the sustainable management of marine resources often depends on understanding spatial population structure and connectivity (Berger et al., 2017; Ciannelli et al., 2013). Yet, integration of the movement ecology paradigm for many aquatic species has lagged terrestrial counterparts, perhaps due to difficulties collecting fine-scale tracking data in the marine realm (e.g. due to increased tag detection issues for telemetry data) and limitations in obtaining similar per capita electronic tag sample sizes for fish populations compared to terrestrial populations (Crossin et al., 2017; Lowerre-Barbieri et al., 2019). However, the last decade has seen a rapid increase in spatially explicit IPMs for marine resources (Punt, 2019a,2019b).

Spatially explicit IPMs can be classified into two main categories (Berger et al., 2017; Cao, Thorson, Punt, & Szuwalski, 2020): spatiotemporal and spatially stratified. Spatiotemporal applications utilize spatial correlation functions to allow a continuous approximation of spatial dynamics with movement being implicitly or explicitly modelled and estimated (e.g. Cao et al., 2020; Thorson, Jannot, & Somers, 2017). Conversely, spatially stratified approaches discretize the model domain into independent population units or geographic areas (Goethel, Quinn, & Cadrin, 2011)

and utilize box-transfer movement dynamics (i.e., connectivity is approximated by instantaneous movement of animals from one spatial unit to another; Beverton & Holt, 1957) with movement parameters either estimated or fixed. Spatiotemporal approaches are gaining momentum as fishery stock assessment tools (i.e., statistical models for estimating population abundance trends based on observed fishery data), because of the ability to elucidate fine-scale dynamics by fitting data at the scale it was collected (e.g. precise spatiotemporal survey locations recorded by GPS; Cao et al., 2020). However, only a handful of spatiotemporal IPM approaches exist (e.g. Cao et al., 2020). Thus, the spatially stratified box-transfer framework remains the most commonly implemented in stock assessment software with spatial capabilities due to the flexibility to fit the relatively coarse spatial scale of historical fisheries data (e.g. Goethel et al., 2011).

Although spatially stratified population models for marine species have been sporadically applied for the past thirty years (e.g. Quinn, Deriso, & Neal, 1990), only a handful of studies have explored the ability to directly estimate complex age- and/or time-varying connectivity patterns. For instance, McGilliard, Punt, Methot, and Hilborn (2015) simulated ontogenetic movement and revealed that models estimating age-based movement parameters performed best even without a priori knowledge of connectivity patterns. Similarly, Carruthers et al. (2015) demonstrated that complex ontogenetic movement could be reliably estimated for two reef fish in the Gulf of Mexico using a simplified movement functional form and that the spatial IPM was more robust to mis-specified spatial structure than a spatially aggregated IPM. On the other hand, Lee, Piner, Maunder, Taylor, and Methot (2017) determined that naïve spatial models performed no better than spatially implicit (i.e., where spatially varying selectivity is treated as a substitute for spatial areas, known as “areas-as-fleets” models) counterparts when age- and time-varying movement occurred. However, spatially implicit areas-as-fleets models have generally been shown to perform poorly when spatial structure exists (e.g. Hurtado-Ferro, Punt, & Hill, 2014; Punt, Haddon, Little, & Tuck, 2016, 2017) and are not widely recommended in place of spatially explicit IPMs (Punt, 2019a, 2019b). For a simulation study with climate-induced poleward distributional shifts and ontogenetic movement, Hulson, Quinn, Hanselman, and Ianelli (2013) found that models estimating age- and time-varying movement utilizing a scaled random walk performed well. Despite disparate approaches and assumed connectivity dynamics, a unifying conclusion across spatial modelling simulations is that inflexible movement parametrizations (e.g. assuming constant movement or incorrect functional forms) can be more detrimental for spatial models than ignoring movement altogether (Goethel, Legault, & Cadrin, 2015b; Hulson et al., 2013; Ying, Chen, Lin, & Gao, 2011).

In general, a better understanding is required regarding the consequences of ignoring connectivity patterns in IPMs, the performance of spatially stratified IPMs when confronted with complex movement and how to flexibly parametrize movement in spatial IPMs. In this study, we implement a generalized spatial

simulation–estimation framework to explore the robustness of spatially stratified IPM movement parametrizations across a range of simulated connectivity dynamics. Our results give insight on the importance of accounting for spatial dynamics in IPMs, while providing guidance on flexible movement parametrizations that can be utilized when little information exists on population-scale connectivity.

2 | MATERIALS AND METHODS

2.1 | Overview

A spatial simulation–estimation framework was utilized to model the dynamics of a metapopulation consisting of two populations with varying demographics and productivity regimes connected through post-settlement movement. The operating model (OM), representing the true dynamics of the system, was parametrized to simulate the dynamics of a relatively short-lived (maximum age of eight years), fast-growing species. Simulations were not meant to mimic the dynamics of any specific species, but were set up to resemble general biological dynamics that may apply to several species groups (e.g. tuna, ground fish, reef fish or coastal pelagic species). The OM simulated a range of connectivity dynamics and was used to generate pseudo-data. Various movement parametrizations within a spatially stratified IPM were then applied to explore bias in important conservation quantities used for providing management advice (e.g. spawning biomass, fishing mortality and recruitment). This work represents an extension of the simulation–estimation framework of Goethel et al. (2019) with a wider diversity of simulated movement scenarios and movement parametrizations in the IPM. The modelling framework is summarized below with a focus on novel movement dynamics. Primary OM parameter values and resulting population trajectories can be found in the Tables S1–S3 and Figures S1–S3. For a full detailed description of the general modelling framework, see Goethel et al. (2019) and the accompanying supplementary material to that publication. The model was coded in AD Model Builder (Fournier et al., 2012) and can be downloaded from the GitHub repository (<https://github.com/dgoethel/Spatial-Assessment-Simulator>).

2.2 | Operating model

The sequential order of events in the OM, which assumed a yearly time step (y), involved: (a) spawning; (b) birth and settlement (recruitment to the populations); (c) release of tagged fish, if tagging takes place in that year; (d) instantaneous movement of tagged and untagged fish between populations; and (e) continuous natural mortality and removals due to harvest throughout the year, including tag recaptures. The main parameters that defined the population trajectories (i.e., fishing mortality, recruitment and movement) all included stochasticity to better incorporate

variability in critical population processes typical of real-world applications. Abundance (N) at age (a) by population (p or j) was projected forward for 30 years starting from input initial abundance at age. Abundance at age was calculated at the beginning of the year (y) before movement occurred (N_{BEF}) based on the abundance after movement (N_{AFT}) in the previous year and age discounted for mortality processes:

$$N_{p,y,a,BEF} = N_{p,y-1,a-1,AFT} e^{[-(F_{p,y-1,a-1} + M_p)]}. \quad (1)$$

Natural mortality (M ; instantaneous rate) was population-specific, but age-invariant and occurred continuously for the entire year. Fishery selectivity (v_i ; susceptibility to the fishing gear) assumed a logistic function with age (Figure S1) and was time-invariant. The yearly fishing mortality multiplier (\bar{F} ; yearly harvest level as an instantaneous rate) assumed a dome shape over time, which was meant to represent a typical fishery development scenario, and one fishery per population was modelled. The total fishing mortality (F) on a given age was the combination of selectivity at age, the yearly harvest rate, and a lognormally distributed annual random deviate (ϵ_F) controlled by the fishing mortality variance term ($\sigma_F = 0.3$):

$$F_{p,y,a} = v_{f,p,a} \bar{F}_{p,y} e^{(\epsilon_{F_{p,y}} - 0.5\sigma_F^2)}; \epsilon_{F_{p,y}} \sim N(0, \sigma_F^2). \quad (2)$$

Connectivity utilized the box-transfer method, which assumed movement was a Markov process. The movement parameter, $T_{y,a}^{j \rightarrow p}$, represented the fraction of age a fish from population j in year y that moved to population p . The simulated movement dynamics for each OM scenario are qualitatively described in the following section ("Movement Dynamics"), whereas the full mathematical descriptions can be found in the Section S1 "Operating Model Movement Parametrization". Abundance after movement was given by:

$$N_{p,y,a,AFT} = j \sum \left[T_{y,a}^{j \rightarrow p} N_{j,y,a,BEF} \right]. \quad (3)$$

Spawning biomass (S) at the beginning of the year was the product of abundance, maturity (m) and weight (w) for mature ages (Figure S1), $a \geq 2$:

$$S_{p,y} = \sum_{a=2}^A N_{p,y,a,BEF} W_{p,a} m_{p,a}. \quad (4)$$

New births were then assumed to be a density-dependent function of spawning biomass based on a Beverton-Holt stock-recruit relationship with lognormally distributed annual random deviations (ϵ_R) controlled by the recruitment variance term ($\sigma_R \sim 0.5$):

$$N_{p,y,a=1,BEF} = \frac{0.8R_{0,p} h_p S_{p,y-1}}{0.2\Phi_{0,p} R_{0,p} (1-h_p + h_p - 0.2 S_{p,y-1})} e^{\epsilon_{R_{p,y-1}} - 0.5\sigma_R^2}; \epsilon_{R_{p,y-1}} \sim N(0, \sigma_R^2), \quad (5)$$

where R_0 was the unfished virgin recruitment and h (value of 0.7) was the steepness of the stock-recruit relationship (i.e., a measure of productivity of the population; Conn, Williams, & Shertzer, 2010). Φ_0 represented the unfished spawning biomass-per-recruit calculated by:

$$\Phi_{0,p} = \sum_{a=2}^A w_a m_a e^{[-(a-1)M_p]}, \quad (6)$$

The fishery was assumed to operate continuously for the entire yearly time step and catch (C) by population, year and age was calculated using Baranov's catch equation (Hilborn & Walters, 1992):

$$C_{p,y,a} = N_{p,y,a,AFT} \left(1 - e^{[-(F_{p,y,a} + M_p)]} \right) \frac{F_{p,y,a}}{F_{p,y,a} + M_p}. \quad (7)$$

A fishery-independent survey (s) was assumed to occur mid-year ($t_s = 0.5$) where survey catch was calculated assuming a time-invariant logistic survey selectivity function (v_s) and a constant catchability scalar (q_s):

$$C_{s,p,y,a} = q_{s,p} v_{s,p,a} N_{p,y,a,AFT} e^{[-(F_{p,y,a} + M_p)t_s]}. \quad (8)$$

The associated expected value of the index of biomass (I) was calculated from:

$$I_{s,p,y} = a \sum (C_{s,p,y,a} w_{p,a}). \quad (9)$$

A multiyear Brownie tag-recovery model (Brownie, Hines, Nichols, Pollock, & Hestbeck, 1993) was also simulated. In each year of the simulation, a new tag cohort could be released into the population, where a cohort (l) was defined by the combination of year, age and population of release. During each release event, 5,000 tags were released, which represented a common average value for conventional tagging programs. For the majority of simulations, tag release frequency was every five years (see next Section 2.5 *Sensitivity Runs* for alternate designs). Based on the results of Goethel et al. (2019), this design provided a cost-effective and realistic tagging protocol (as opposed to yearly tagging). A tagged individual was assigned to a release cohort by apportioning the total releases to a population based on the relative survey biomass and distributing across ages within a population relative to survey age compositions. The tag deployment dynamics were parametrized such that the number of tag releases was much less than 1% of initial population abundance (i.e., only a small fraction of the population was tagged as in any real-world application). Tag abundance (n) by cohort was calculated identically to the main population (i.e., following Equations 1-3), but with recruitment replaced by tag release events. Cohort-specific recaptures (r) were calculated using Baranov's catch equation adjusted to account for population-specific, time-invariant tag reporting rate (β):

$$r_{p,y,a}^l = n_{p,y,a,AFT}^l \cdot \beta_p \frac{F_{p,y,a} \left(1 - e^{[-(F_{p,y,a} + M_p)]} \right)}{F_{p,y,a} + M_p}. \quad (10)$$

A list of OM inputs and values can be found in the Table S1.

2.2.1 | Movement dynamics

Four movement dynamics were simulated (Figure 1; see the Section S1 “Operating Model Movement Parametrization” for a full description of the equations and parameter values governing movement in the model). The density-dependent (*DD*) formulation assumed that fish emigrated with increasing probability as abundance approached the age-specific carrying capacity term in a given population (Goethel et al., 2015b, 2019). Connectivity varied most strongly across years (without any long-term directional trend), but age-based patterns were also present (Figure S2; Table S2). In the ontogenetic (*ONT*) OM, age-based movement patterns were implemented to resemble movement from juvenile (population two) to adult (population one) habitat as fish became older. Younger fish (i.e., ages one through four) had a high probability of moving to and remaining in population two, whereas older fish (ages five and older) had a high probability of moving to and remaining in population one. The climate-induced movement (*CLM*) OM emulated a poleward (or deeper) distributional shift where fish developed increasing affinity for the environmental

conditions of population one. Similar patterns of age-based movement as the *DD* OM were used, but a time trend was incorporated that increased the probability of fish moving to, and remaining in, population one over the time series (e.g. Link et al., 2011). Although no other biological characteristics were linked to the time trend (i.e., improved biological conditions in population one were not directly simulated), population one was characterized by generally more favourable biological parameters (i.e., a higher R_0 and slightly lower natural mortality; Table S1) in all scenarios. Finally, the climate-induced time trends were combined with the ontogenetic age-based movement patterns (*C+O* OM). The *C+O* OM demonstrated how climate impacts on ontogenetic migration patterns might influence relative population distributions and trajectories (e.g. Barbeaux & Hollowed, 2018).

For all movement scenarios, random variation was included by multiplying the emigration rate by a lognormally distributed random deviation controlled by the movement variance term ($\sigma_T = 0.3$; with the same realized set of random numbers generated for each OM movement scenario) and bounds implemented to ensure movement rates remained between zero and one (see the Supplementary Material for a full description of the simulated movement dynamics). The random number used to define a given deviation was population,

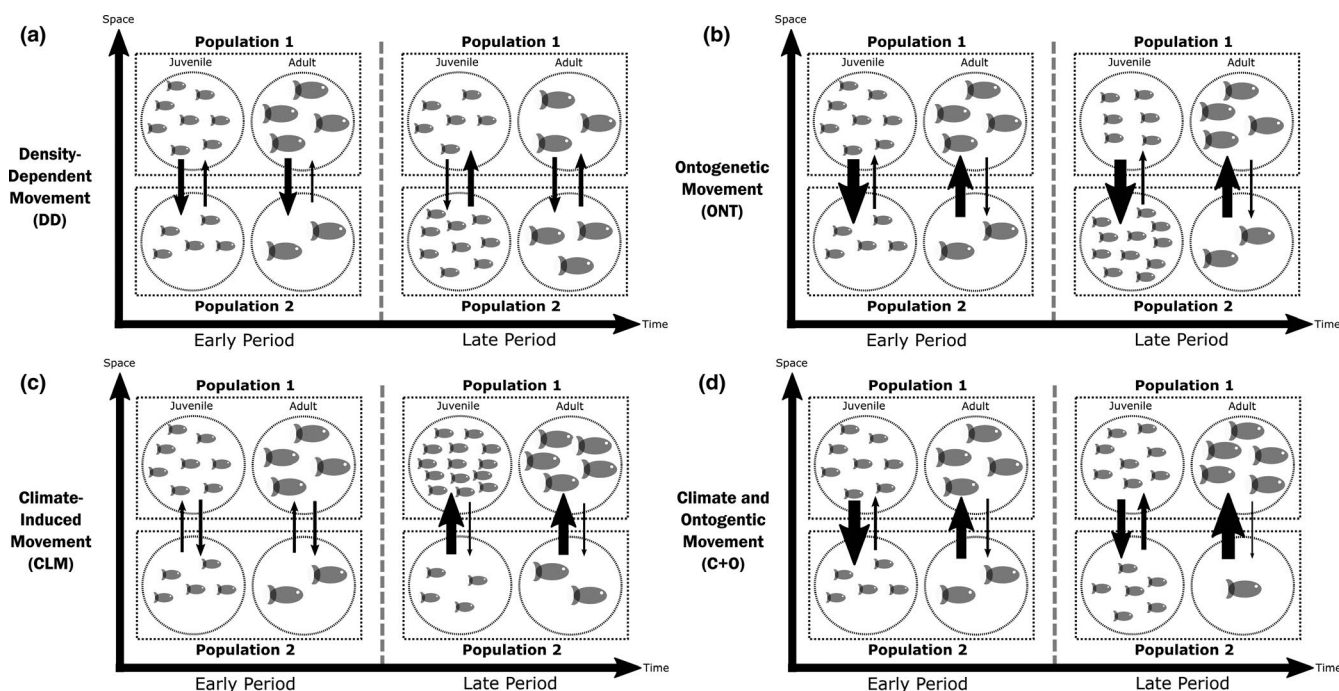


FIGURE 1 Schematic representation of the four simulated movement scenarios implemented in the operating model (OM). Although age- and time-varying movement are implemented in all movement scenarios (see Figure S2), for simplicity of the figure ages are grouped into juvenile (ages one through four) and adult (ages five through eight) phases whereas time variation is grouped by early (first fifteen years) and late (recent fifteen years) periods. The level of movement (arrows) among populations (dotted rectangles) is indicated by arrow thickness. For the density-dependent (*DD*) scenario (a), emigration increases as a population becomes more densely populated, and the rate of emigration varies over time as new recruits enter each population and older fish redistribute across the populations. With ontogenetic (*ONT*) movement (b), younger fish are more attracted to population two (e.g. it represents juvenile habitat), while older fish are more attracted to population one (e.g. it represents spawning habitat), and these affinities do not vary strongly over time. In the climate-induced movement (*CLM*) scenario (c), fish have an increasing affinity over time for population one (e.g. emulating climate impacts that improve the environmental conditions in population one); both emigration from population two and residency in population one increase over the time series. Finally, the climate and ontogenetic (*C+O*) scenario (d) overlays the age-based movement patterns of b with the climate-induced time trend in c.

TABLE 1 Names and convergence rates for the twenty-four combinations of the four OM movement scenarios and the six IPM movement parametrizations

OM movement	IPM movement parametrization	Identifier	Convergence rate
Density-dependent (<i>DD</i>)	No movement (<i>NO_T</i>)	<i>DD_NO_T</i>	0.976
	Constant (<i>CNST</i>)	<i>DD_CNST</i>	1.000
	Age-varying (<i>AGE</i>)	<i>DD_AGE</i>	1.000
	Time-varying (<i>YR</i>)	<i>DD_YR</i>	1.000
	Movement estimated in two-year time blocks and for every two ages (<i>2YR+2AG</i>)	<i>DD_2YR+2AG</i>	1.000
	Time- and age-varying (<i>YR+AG</i>)	<i>DD_YR+AG</i>	1.000
Ontogenetic (<i>ONT</i>)	No movement (<i>NO_T</i>)	<i>ONT_NO_T</i>	1.000
	Constant (<i>CNST</i>)	<i>ONT_CNST</i>	1.000
	Age-varying (<i>AGE</i>)	<i>ONT_AGE</i>	0.984
	Time-varying (<i>YR</i>)	<i>ONT_YR</i>	0.936
	Movement estimated in two-year time blocks and for every two ages (<i>2YR+2AG</i>)	<i>ONT_2YR+2AG</i>	1.000
	Time- and age-varying (<i>YR+AG</i>)	<i>ONT_YR+AG</i>	1.000
Climate-induced (<i>CLM</i>)	No movement (<i>NO_T</i>)	<i>CLM_NO_T</i>	1.000
	Constant (<i>CNST</i>)	<i>CLM_CNST</i>	0.992
	Age-varying (<i>AGE</i>)	<i>CLM_AGE</i>	0.988
	Time-varying (<i>YR</i>)	<i>CLM_YR</i>	0.992
	Movement estimated in two-year time blocks and for every two ages (<i>2YR+2AG</i>)	<i>CLM_2YR+2AG</i>	0.998
	Time- and age-varying (<i>YR+AG</i>)	<i>CLM_YR+AG</i>	0.988
Climate-induced and ontogenetic (<i>C+O</i>)	No movement (<i>NO_T</i>)	<i>C+O_NO_T</i>	1.000
	Constant (<i>CNST</i>)	<i>C+O_CNST</i>	0.992
	Age-varying (<i>AGE</i>)	<i>C+O_AGE</i>	0.998
	Time-varying (<i>YR</i>)	<i>C+O_YR</i>	1.000
	Movement estimated in two-year time blocks and for every two ages (<i>2YR+2AG</i>)	<i>C+O_2YR+2AG</i>	1.000
	Time- and age-varying (<i>YR+AG</i>)	<i>C+O_YR+AG</i>	1.000

year and age specific, which allowed for moderate random variation across all axis of movement even when the primary drivers were single factors (e.g. age or time). The age and time-varying movement rates are shown in Figure S2 with corresponding movement parameters provided in Table S2, while the resulting population trajectories for each of the movement OMs are illustrated in Figure S3.

2.2.2 | Simulated data

The model produced five sets of population-specific pseudo-data: (a) age compositions from the catch; (b) survey age compositions; (c) total yield (i.e., the summation across ages of the product of catch and weight); (d) survey biomass; and (e) tag recaptures. Pseudo-data were generated for each year of the model with measurement error simulated for each data source using stochastic processes based on an assumed underlying probability distribution (Table S3). For the tagging data, a multinomial probability distribution was utilized, but

the effective sample size was set at 200 which was much lower than the actual number of tags released per cohort (i.e., 5,000 tags). The lower effective sample size allowed for increased uncertainty (i.e., implicit overdispersion) in the tagging data; otherwise, the tagging data would have been overly informative and not representative of real-world observations. For each movement OM scenario, 500 pseudo-datasets were simulated. The error levels along with the number of runs were chosen to adequately encapsulate stochasticity and represent typical levels of variation observed in aquatic populations and associated data collection.

2.3 | Integrated Population Models

Spatially stratified IPMs were fit to the thirty-year time series of pseudo-data for each of the movement OMs. With the exception of movement parametrization, the IPM structure matched that of the OM including fixing steepness, natural mortality and reporting

TABLE 2 Median absolute relative error (MARE) in estimates of terminal year spawning stock biomass

EM Movement parametrization	Density-dependent (DD) OM		Ontogenetic (ONT) OM		Climate (CLM) OM		Climate and Ontogenetic (C+O) OM				
	Population 1	Population 2	Population 1	Population 2	Population 1	Population 2	Population 1	Population 2			
NO_T	11.34	14.61	6.23	9.63	29.16	16.25	10.87	16.25	8.95	33.34	7.59
CNST	5.50	5.14	2.98	36.15	16.51	118.30	33.73	118.30	6.58	61.23	22.88
AGE	5.85	5.21	3.14	4.53	4.79	120.40	34.22	120.40	15.91	43.47	4.70
YR	5.38	5.22	2.98	77.54	39.23	12.97	6.28	12.97	55.02	47.24	21.69
2YR+2AG*	5.08	5.43	3.01	5.56	5.87	29.24	13.51	29.24	4.50	6.93	3.27
YR+AG	4.55	4.71	2.97	11.59	5.82	87.29	28.84	87.29	5.83	20.22	4.30

Note: The largest MARE value for each IPM (across a row) is denoted in bold italics. The lowest MARE within each movement OM (down a column) is highlighted in light grey. Dark grey shading denotes the min-max solution (i.e., the IPM with the lowest maximum MARE across all movement OMs).

rate (although a sensitivity run was performed with reporting rate estimated, see below) at the true values. A maximum-likelihood estimation (MLE) framework was utilized to estimate population-specific parameters (e.g. yearly fishing mortality, R_0 , yearly recruitment deviations, time-invariant logistic selectivity parameters, initial abundance at age and movement rates) where all parameters were treated as fixed effects. MLE variance terms (σ ; i.e., the assumed standard deviations associated with the lognormally distributed data sources, as well as the equivalent value used to penalize deviations from the stock-recruit function) and effective sample size (ESS; for multinomial distributions) for each likelihood component were taken directly from the operating model (Table S3). Penalty functions were utilized to stabilize estimates and prevent unfeasible parameter values (e.g. zero values of virgin recruitment, extremely high levels of movement or fishing mortality and large recruitment deviations).

Variants of the IPM included the following parametrizations of movement (Table 1): (a) fish were not allowed to move among populations (NO_T); (b) population-specific age- and time-invariant movement rates were estimated (CNST); (c) movement was estimated for each age and population (AGE); (d) time-varying movement rates were estimated for each population (YR); (e) movement rates were estimated in two-year time blocks and for every other age for each population (2YR+2AG); and (f) movement was freely estimated for every year and age for each population (YR+AG). Additionally, two variations of each of these IPMs were developed: the first estimated population-specific reporting rate (Est_B); the second fixed movement at the true values from the OM (FIX_T; see section 2.5 Sensitivity Runs and Table S4 for more information on each).

2.4 | Evaluation of Model Performance

The performance of each IPM was compared based on bias and precision in estimates of population parameters. Time series plots of percent relative error (RE) in population-specific and total spawning biomass, fishing mortality (population-specific values only) and recruitment were developed to explore estimation performance over time. Additionally, the median absolute relative error (MARE; a combined measure of bias and variability) across all 500 pseudo-datasets for population-specific spawning biomass in the terminal year was calculated by:

$$MARE_{p,y=30}^S = median \left(\left| RE_{1,p,y=30}^S \right|, \dots, \left| RE_{500,p,y=30}^S \right| \right). \quad (11)$$

The MARE was used to determine the “min-max” solution, which identified the best-performing IPM movement parametrization across the range of simulated movement OMs. The min-max solution involved identifying which IPM configuration had the smallest maximum value of MARE across all OMs (McGilliard et al., 2015). The min-max solution provided guidance on which movement estimation approach was most robust to uncertainty in movement dynamics. Model stability, an indicator of overparametrization and robustness, was determined based on the convergence rate.

2.5 | Sensitivity Runs

A number of sensitivity runs were developed to explore the robustness of the IPMs and conclusions of the analyses. An additional OM scenario (*No_Move*) was simulated with closed populations (i.e., no movement) to determine whether IPMs were able to adequately account for negligible emigration. To examine the impact of data availability, OMs were developed that simulated either no tagging data (*NO_TAG*) or yearly tagging (*TAG_YR*). The former OM represented a common data limitation for marine resources where auxiliary information may not be available, while the latter illustrated an ideal data situation. Two alternate life-history OMs were developed, which included a short-lived (*SL*) and long-lived (*LL*) variant. The long-lived OM doubled the number of ages (to sixteen), the age at 50% maturity, and the age at 50% selectivity, while halving the natural mortality. On the other hand, the short-lived OM halved the number of ages (to four), the age at 50% maturity and the age at 50% selectivity, whereas natural mortality was doubled. Although the life-history OMs were rudimentary approximations of either fast-growing small pelagic species or relatively slow growing ground fish or deep-water species, they provided insight into how the IPMs performed with variable life-history dynamics, particularly for estimation of age-based movement rates.

Although incorporation of tag data within an IPM can be beneficial for aiding the estimation of movement and mortality parameters, its inclusion also necessitates further model assumptions or estimated parameters (e.g. tag shedding, mortality and reporting rate; Goethel et al., 2019; Vincent, Brenden, & Bence, 2017, 2020). Because the IPMs assumed, unrealistically, that tag reporting rate was known precisely (i.e., fixed at the true value), sensitivity runs were performed with population-specific reporting rates directly estimated to determine if the added estimated parameters led to increased bias or imprecision (*Est_B*). Finally, each of the IPMs was run with movement fixed at the true value from the OM (*FIX_T*), which represented a pseudo self-consistency run demonstrating whether movement or other parameters were the primary source of uncertainty in the model. Results from sensitivity runs were provided in the Supplementary Material and discussed briefly in the following section (see Table S4 for a complete list of sensitivity runs presented and Figures S10–S16 for the results from these runs).

3 | RESULTS

3.1 | Best-Performing IPM Parametrizations

All models demonstrated high convergence rates (i.e., greater than 90%; Table 1) indicating that none of the models had any major parameter confounding or model stability issues. Depending on the simulated movement, a different IPM demonstrated the best performance based on MARE in terminal spawning biomass (Table 2). The best-performing IPM tended to be the one that could parsimoniously estimate the primary driver of the movement dynamics

(e.g. estimating age-varying trends for ontogenetic movement or time-varying trends for climate-induced movement). For each of the movement OMs, the best-performing IPMs demonstrated generally unbiased and relatively precise estimation of population-specific spawning biomass and fishing mortality over the entire time series (Figures 2–3). But, recruitment estimates, although generally median unbiased, were highly imprecise (Figure S4). The impacts of time trends in movement (i.e., the *CLM* and *C+O* OMs) were the most problematic to interpret for the IPMs, which resulted in slight trends in bias over time (Figures 2–3). Inclusion of tagging data was extremely helpful for reducing these bias trends, but the interplay between the tag release frequency (i.e., release events every five years) and the accuracy of subsequent mortality and movement parameter estimates resulted in a cyclical bias in these parameters and associated spawning stock biomass and fishing mortality (Figures 2–3, Figure S5; see 3.3 *Sensitivity Runs* for an explanation of this phenomenon).

The *2YR+2AG* parametrization proved to be the most robust to the various movement OMs (i.e., it was the min-max solution), providing the lowest maximum MARE (maximum value of 29.24 for terminal spawning biomass in population two for the *CLM* OM; Table 2). The *2YR+2AG* parametrization was also chosen as the min-max solution when exploring MARE across the entire time series (Table S5). Although the *2YR+2AG* parametrization demonstrated limited bias for most of the movement OMs, it exhibited increasing bias for the last ten years of the time series under the *CLM* scenario (Figure S6). Increasing bias for the *CLM* scenario was a common theme across IPM parametrizations, including the best-performing *YR* IPM (Figure S7). The unidirectional nature of movement under the *CLM* OM likely resulted in difficulty disentangling population-specific signals in the data, especially regarding recruitment, leading to the increasing bias seen in many of the IPMs. Conversely, when time and age trends in movement were simulated simultaneously (*C+O* OM), the *2YR+2AG* parametrization demonstrated limited bias with no time trends, despite the comparatively more complex simulated dynamics compared to the *CLM* OM (Figure S7–S8).

3.2 | Detriments of Ignoring or Oversimplifying Movement

Ignoring movement dynamics (i.e., applying the *NO_T* IPM) was highly detrimental to obtaining unbiased estimates of population-specific spawning biomass and fishing mortality, with median absolute bias ranging from 10% – 100% across OMs (Figures 4–5). Similar trends in bias but with higher imprecision were observed in estimates of recruitment (Figure 6 and Figure S9). Strong age-based movement patterns were the most problematic when movement was ignored in the IPM (Figures 4–5). On the other hand, the *NO_T* IPM demonstrated limited bias in estimates of spawning biomass for the *CLM* OM, but bias increased rapidly in the terminal five years resulting in similar bias levels as the *2YR+2AG* IPM (Figure 6). Under the *CLM* scenario, the *NO_T* IPM also demonstrated a strong time trend in recruitment bias. The model increasingly overestimated recruitment

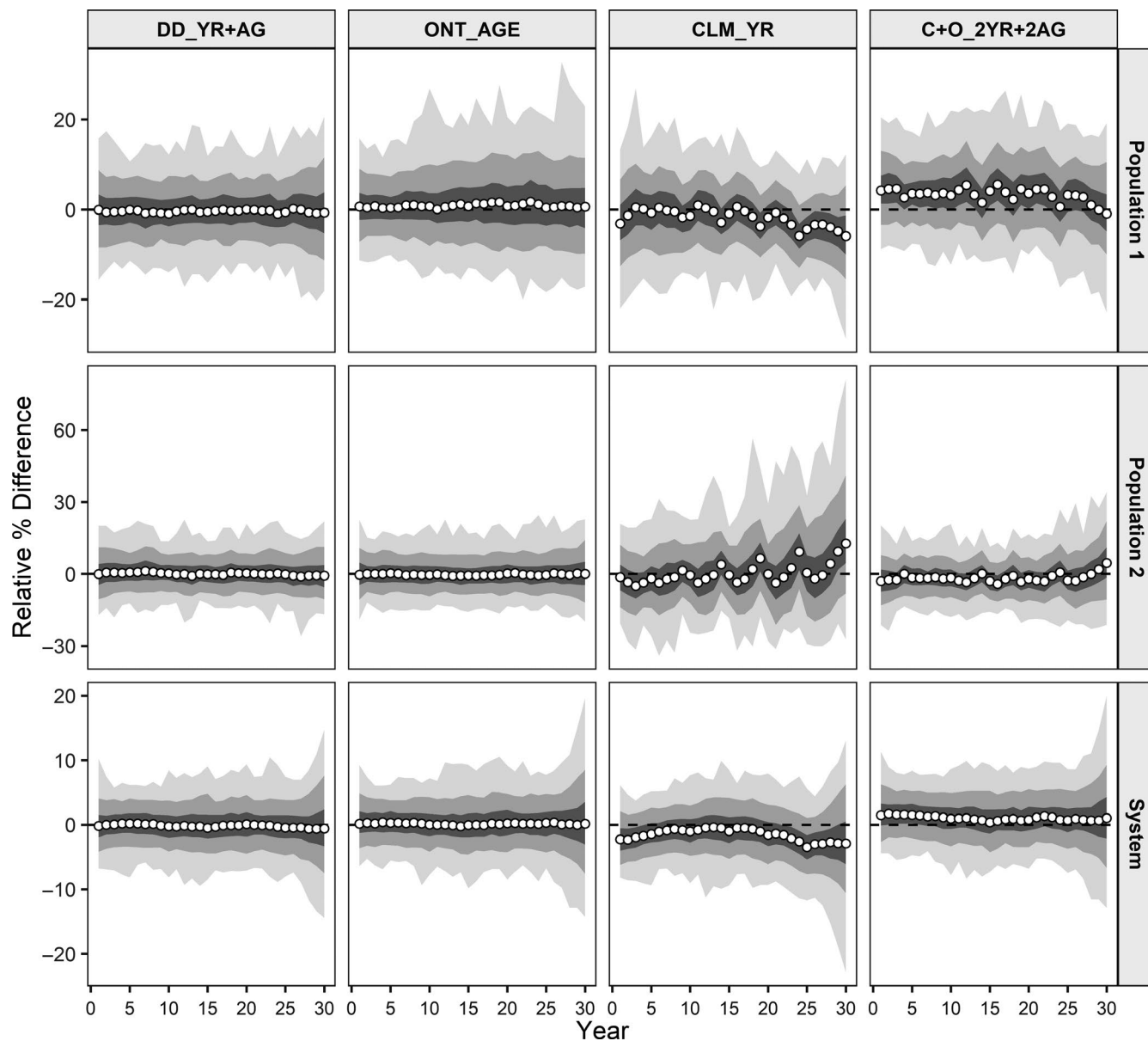


FIGURE 2 Time series of bias (relative percent difference) in population-specific and system-wide spawning biomass for the best-performing (as determined by the lowest MARE; Table 2) IPM for each movement OM. Corresponding simulation intervals are provided by the various fill colours (i.e., 100% in light grey, 95% in medium grey, and 75% in dark grey). White dots illustrate median bias. The dashed line indicates zero bias. The combination of OM and IPM names are given as column headers and described in Table 1

in population one and underestimated recruitment in population two, because the model was attempting to account for the increasing emigration rate of fish out of population two over the time series (Figure 6).

Implementing oversimplified movement parametrizations was often as detrimental to IPM performance as assuming no movement. For instance, the *NO_T* IPM outperformed the *CNST* IPM for all simulated movement scenarios except for the *DD* OM, with the *CNST* IPM exhibiting a worse min-max performance for both terminal year and aggregate MARE (e.g. largest MARE value for terminal SSB of 118.3 compared to 33.34 for the *NO_T* IPM; Table 2 and Table S5). Perhaps surprisingly, the *AGE*, *YR* and *YR+AG* IPMs also demonstrate higher maximum MARE values for terminal SSB than the *NO_T* IPM

(Table 2). However, only the *YR* IPM maintained higher maximum MARE values than the *NO_T* IPM for SSB when the estimates across the entire time series were considered (Table S5). Furthermore, the *YR+AG* IPM performed similarly to the *2YR+2AG* IPM (with the exception of extremely poor performance when the *YR+AG* IPM was applied to the *CLM* OM), especially when complex movement was present (e.g. the *C+O* OM; Table 2 and Table S5; Figures S7–S8). Contrariwise, despite being the best models when correctly specified, the *AGE* and *YR* IPMs often performed worse than the *NO_T* IPM when the primary driver of movement was ignored (e.g. applying the *YR* IPM to the *ONT* OM; Table 2 and Table S5; Figures S7–S8). Thus, our results suggest that it was generally better to implement movement parametrizations that were likely to be slightly

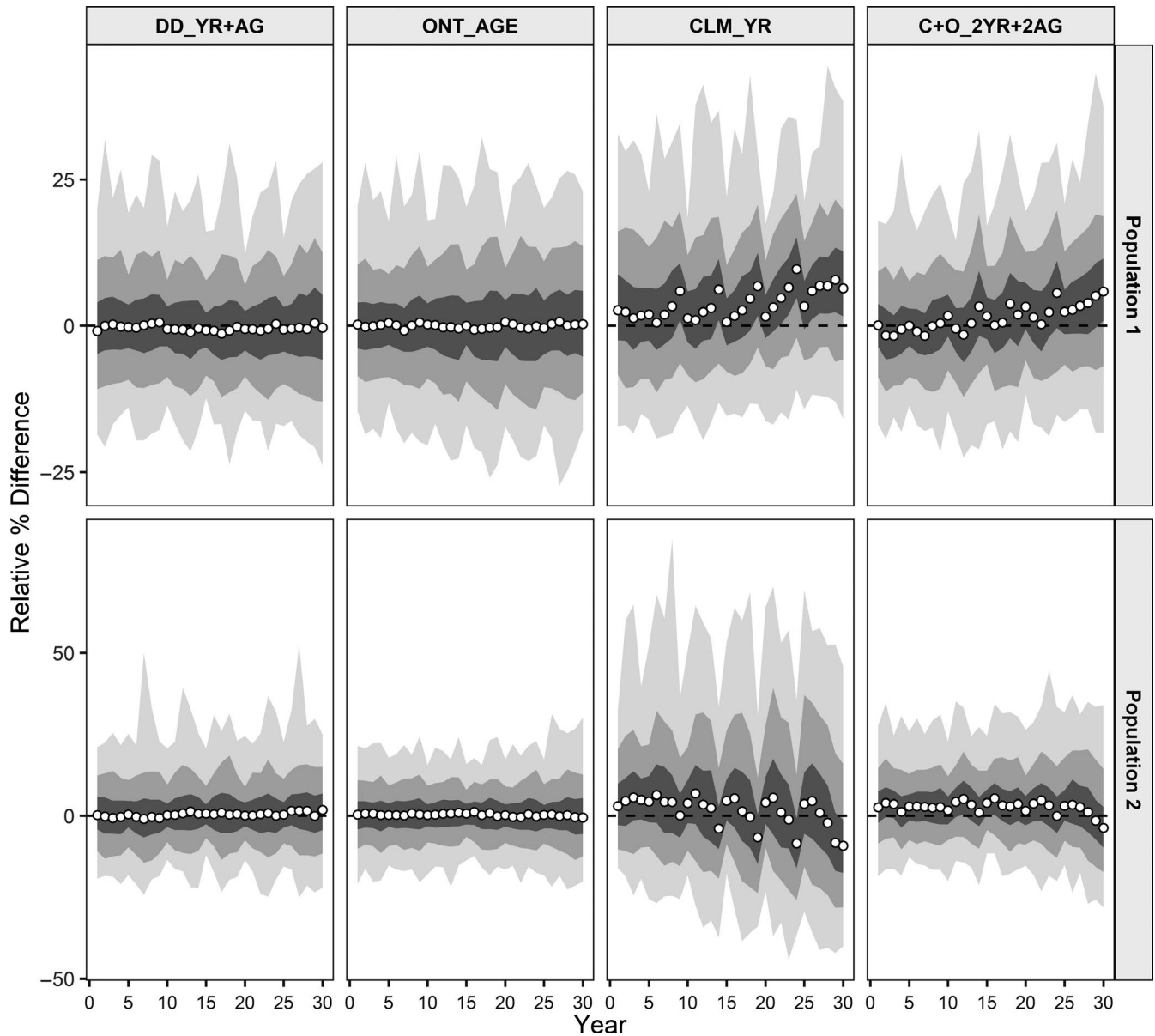


FIGURE 3 Time series of bias (relative percent difference) in population-specific fishing mortality (on fully selected ages) for the best-performing (as determined by the lowest MARE; Table 2) IPM for each movement OM. Corresponding simulation intervals are provided by the various fill colours (i.e., 100% in light grey, 95% in medium grey, and 75% in dark grey). White dots illustrate median bias. The dashed line indicates zero bias. The combination of OM and IPM names are given as column headers and described in Table 1

more complex than the true dynamics compared to oversimplifying or ignoring movement. However, careful consideration of the potential tradeoffs between overparametrization and precision should be considered (i.e., the 2YR+2AG model was more parsimonious and outperformed the YR+AG IPM).

3.3 | Sensitivity Runs

All of the IPMs were robust to negligible movement rates (i.e., the closed population assumption) of the *No_Move* OM scenario (Figure S10). However, the impact of overparametrization was seen in the more complex movement estimation models (Figure S10). Estimation

bias increased in the terminal five years for the *AGE*, *YR*, *2YR+2AG* and *YR+AG* IPMs, which was likely due to the limited information on recruitment from the age composition data in these years leading to increased movement and recruitment parameter correlation. However, bias was typically less than 5% and was insignificant compared to ignoring or misdiagnosing movement when it was actually occurring (Figures 4-5).

The strong influence of tagging data was discernible in the cyclical bias patterns observed in spawning biomass and fishing mortality for the best-performing IPMs under the *CLM* and *C+O* OMs (Figures 2-3). During and immediately following tag release events, estimation of movement parameters improved causing a sharp decrease in bias (Figure S5) resulting in the observed patterns in

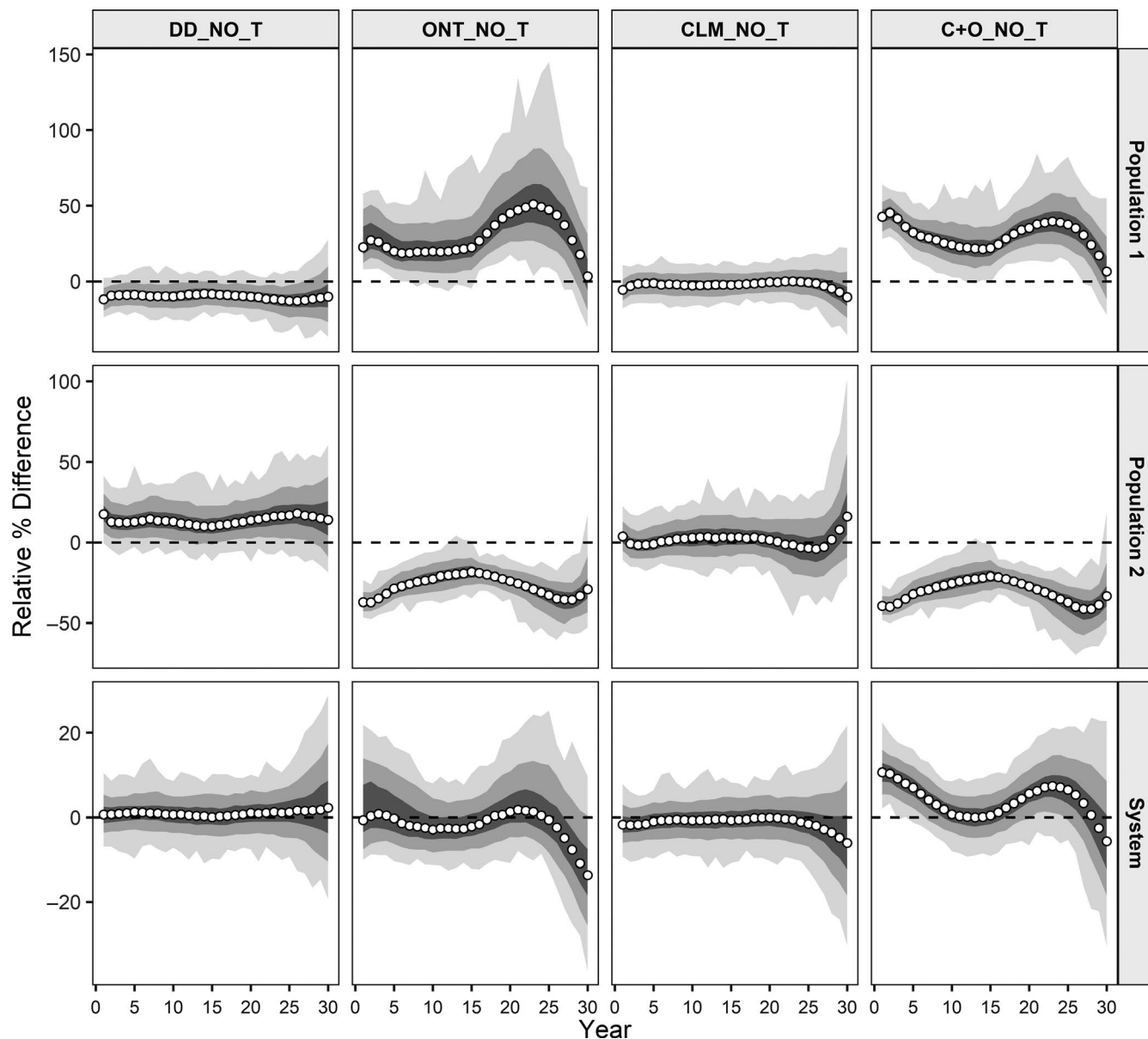


FIGURE 4 Time series of bias (relative percent difference) in population-specific and system-wide spawning biomass when movement is ignored (*NO_T*) in the IPM for each movement OM. Corresponding simulation intervals are provided by the various fill colours (i.e., 100% in light grey, 95% in medium grey, and 75% in dark grey). White dots illustrate median bias. The dashed line indicates zero bias. The combination of OM and IPM names are given as column headers and described in Table 1

population trajectory bias. When yearly tagging data were available (*TAG_YR* scenarios), bias levels decreased and the pattern disappeared (Figure S11). Yearly tagging data was particularly helpful in reducing the bias observed under the *CLM* scenario (Figures S7 and S11). Without tagging data (*NO_TAG* scenarios), IPMs demonstrated increased bias and a twofold decrease in precision (Figures S12–S13). When time trends in emigration existed (e.g. the *CLM* and *C+O* scenarios) and no tagging data were available, IPMs had difficulty interpreting the signals in the data (Figure S12). For instance, with the *CLM* OM, the *YR* IPM demonstrated increasing bias levels across the time series when no tagging data were available to aid estimation of emigration rates. However, inclusion of tagging data appeared to be less important for the estimation of age-based movement (i.e., when

it was the only main source of movement variation as in the *ONT* OM; Figure S13).

Results were consistent across different life-history types, but imprecision in spawning biomass increased when there were more ages (i.e., the *LL* OM) for which to estimate movement parameters (Figure S13). On the other hand, convergence rates diminished for the *SL* OM (Table S4), likely due to the decrease in data (i.e., ages in age composition and tagging states) from which to estimate parameters.

The IPMs were generally able to estimate the population-specific reporting rate (*Est_B* IPMs) with limited bias and resulting in only minor increases in uncertainty and bias in spawning stock biomass trajectories (Figure S14–S15). When movement in the IPM was fixed

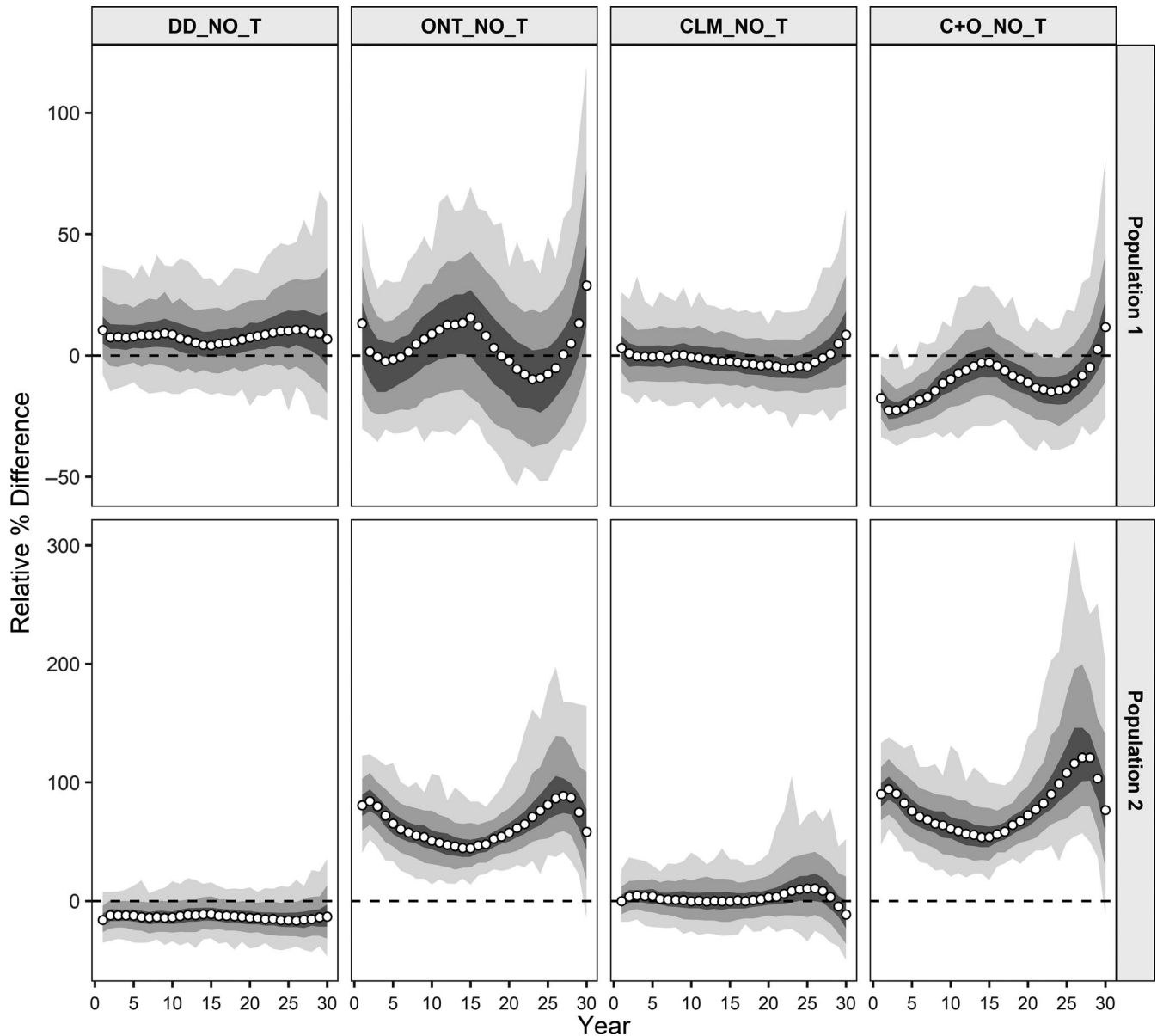


FIGURE 5 Time series of bias (relative percent difference) in population-specific fishing mortality (on fully selected ages) when movement is ignored (NO_T) in the IPM for each movement OM. Corresponding simulation intervals are provided by the various fill colours (i.e., 100% in light grey, 95% in medium grey, and 75% in dark grey). White dots illustrate median bias. The dashed line indicates zero bias. The combination of OM and IPM names are given as column headers and described in Table 1

at the true value from the OM (FIX_T IPMs), bias in spawning stock biomass essentially disappeared and precision increased dramatically, which demonstrated that difficulty estimating movement rates was the primary source of uncertainty in the model (Figure S16).

4 | DISCUSSION

Understanding spatial variability and movement in animal populations is imperative for determining a species' response to dynamic processes, such as climate-induced changes and harvest mortality (Allen & Singh, 2016; Zipkin & Saunders, 2018). The interaction of animal movement, the spatiotemporal distribution of harvesters

and implementation of spatial conservation measures often lead to disproportionate and unintuitive impacts on spawning components within a population network, which cannot be predicted by spatially aggregated models (Fu & Fanning, 2004). For instance, in our model, redistribution among populations due to different movement patterns when comparing the CLM and ONT OMs led to an almost twofold increase in total system spawning biomass mostly due to the minor differences in fishing mortality and selectivity by population (Figure S3). Similarly, as illustrated by Link et al. (2011) and demonstrated with the CLM OM, when unidirectional distribution shifts occur, a spatially aggregated population model would likely predict rebuilding throughout the species range, while being naïve to the potential decline of the population

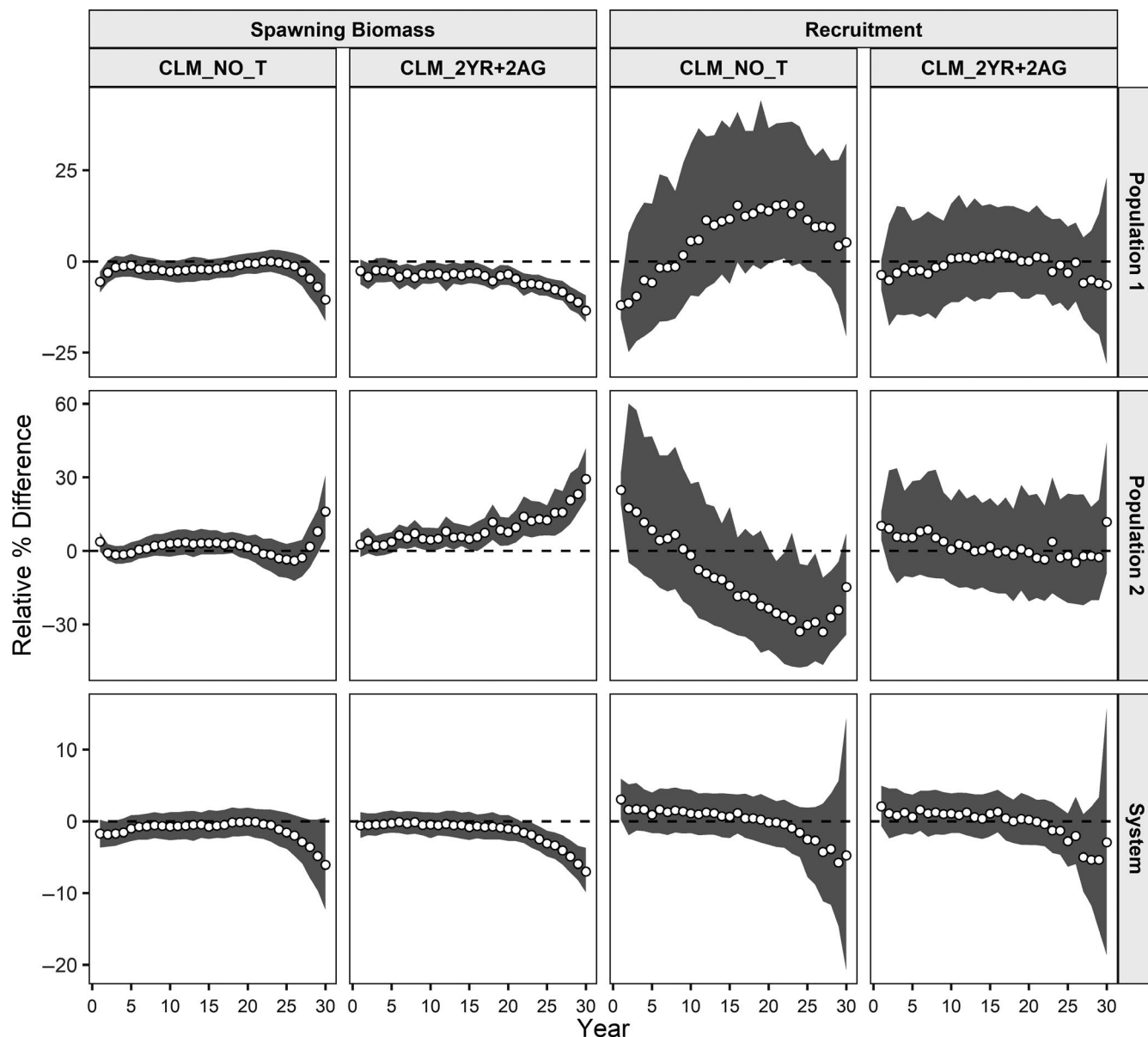


FIGURE 6 Time series of bias (relative percent difference) in population-specific and system-wide spawning biomass and recruitment for the no movement (*NO_T*) and the *2YR+2AG* (i.e., the min-max solution as determined by the lowest maximum MARE across movement OMs; Table 2) IPMs for the climate-induced movement (*CLM*) OM. Corresponding 75% simulation intervals are provided by the dark grey fill. White dots illustrate median bias. The dashed line indicates zero bias. The combination of OM and IPM names are given as column headers and described in Table 1

undergoing increasing emigration rates (Figure S3). A negative feedback loop between management advice and population size would likely ensue where quotas would be set too high and decreased species resiliency could occur as the population with increased emigration continued to decline (Fu & Fanning, 2004; Punt, 2019a,2019b). Climate-induced distributional shifts could also lead to large segments of the resource moving into areas that are outside the existing spatial domain of fishery surveys, which could further exacerbate bias in IPMs and impede the ability to implement sustainable harvest strategies. Improving the ability of spatially stratified IPMs to accurately detect shifts in a species distribution will help communities that rely on the harvest of the

resource to adequately plan and become resilient to such changes (Badjeck, Allison, Halls, & Dulvy, 2010; Hughes et al., 2012). Similarly, implementation of reserves or protected areas relies on being able to accurately monitor spatiotemporal dynamics of animals and harvesters (White, 2015). Thus, spatially stratified IPMs are warranted to help develop sustainable and well-informed spatial conservation strategies (Berger et al., 2017; Chandler & Clark, 2014; Punt, 2019a,2019b). Furthermore, increased collection and utilization of tagging data, including conventional, electronic and natural tags, can help differentiate whether observed population fluctuations are due to changes in availability or abundance (Saunders et al., 2019), especially as fish distributions begin

to extend beyond the domain of existing data collection regimes (e.g. fishery surveys) due to climate-induced poleward (or deeper) movement.

We demonstrated the ability of spatially stratified IPMs to account for complex movement patterns and accurately estimate population-specific biomass levels. Results indicate that using flexible parametrizations of movement is warranted to avoid oversimplifying connectivity dynamics, which may cause estimation bias on par with ignoring movement completely (Goethel et al., 2015b; Hulson et al., 2013; Lee et al., 2017). However, the flexibility in parametrizing both age- and time-varying connectivity must be balanced against the number of parameters to be estimated (i.e., weighing complexity versus parsimony). For instance, binning movement parameters in two-year and two-age blocks (i.e., the 2YR+2AG IPM) was the most robust across simulated movement OMs. Although the IPM that solely estimated movement parameters for the primary driver of connectivity dynamics in the OM often performed best (i.e., estimating age-based movement for the ontogenetic OM and yearly movement for the climate OM), the 2YR+2AG IPM was often able to adequately account for both age- and time-varying movement when completely naïve to the underlying true connectivity.

However, when confronted with the increasingly unidirectional movement rates associated with the climate change (CLM) scenario, the 2YR+2AG IPM performed relatively poorly. Conversely, the IPM that ignored movement (NO_T) performed adequately for the CLM scenario. Yet, both the NO_T and 2YR+2AG IPMs demonstrated increasing bias over the terminal five to ten years of the CLM scenario resulting in similar bias levels over this time period (Figure 6). The NO_T IPM was only able to adjust for the inability to estimate movement by overestimating the recruitment in population one and underestimating it in population two. Similarly, estimation difficulties for the spatial IPMs associated with the CLM OM were most likely due to correlation among recruitment and movement parameters (i.e., increasing abundance in population one could be equally explained through increased recruitment in population one, as was the case in the NO_T IPM, or increased rates of immigration into population one). Simultaneously, the unidirectional nature of movement likely led to a lack of contrast in the data (similar to a “one-way trip” in catch data; Hilborn & Walters, 1992) where the signals from the ever-growing population one inundated those from the increasingly smaller population two (i.e., there was limited information content in the data to differentiate the population trajectories and accurately estimate the trends in population two). Difficulty interpreting the productivity of smaller population units in spatial IPMs, is a common issue (e.g. Vincent et al., 2017), but it can sometimes be alleviated through unique tagging study designs (e.g. disproportionately tagging the smaller population unit; Goethel et al., 2019).

Although the NO_T IPM performed comparatively well for the CLM OM, the misinterpretation of spatial productivity could have important implications for implementation of sustainable harvest strategies (Goethel & Berger, 2017). Additionally, unlike the 2YR+2AG IPM, ignoring movement was highly problematic under all other movement scenarios. Therefore, given that the 2YR+2AG IPM

was generally robust to all simulated movement scenarios (including no movement) and demonstrated only slightly worse performance under the CLM scenario, there was no apparent benefit to ignoring movement in the IPM for the scenarios simulated.

Under all movement scenarios, the performance of spatially stratified IPMs was greatly improved by the incorporation of tagging data, which supports conclusions from a wide array of previous simulation studies with tag-integrated models (e.g. Goethel et al., 2015b, 2019; Hulson, Miller, Ianelli, & Quinn, 2011; Hulson et al., 2013; Vincent et al., 2017, 2020). But, inclusion of tagging data must be carefully considered given the caveats associated with its use, such as the need to internally or externally estimate additional parameters (e.g. reporting rate, tag loss, tag mortality and tag mixing) and the reliability or scalability of the tagging data (i.e., is there overdispersion and do tagged animals adequately represent the dynamics of the greater population; Goethel et al., 2019). Additionally, the ability to obtain adequate tag sample sizes (i.e., number of releases in a given release event) may be an issue when funding is limited, for rare species, or those otherwise difficult to tag. Furthermore, when tag loss or tag mortality rates are high, tag-integrated models are likely to be biased if external estimates of these values are inaccurate (Riecke et al., 2019; Vincent et al., 2020). Obtaining adequate recaptures can also be problematic when fishing mortality is low or non-reporting of recaptures is high. Similarly, accurate estimates of spatiotemporal variation in tag reporting rates is critical for achieving unbiased estimates from tag-integrated models, because reporting rates are often highly correlated with fishing mortality and can be difficult to estimate without auxiliary information (Brenden, Jones, & Ebener, 2010; Cadigan & Bratney, 2006; Goethel et al., 2015b; Vincent et al., 2017, 2020). For example, Goethel et al. (2015b) demonstrated that fixing reporting rate at the wrong value led to error levels in a spatially explicit IPM on par with ignoring movement altogether.

Although the limitations must be carefully considered when using tagging data, simulation studies have increasingly demonstrated that issues with tagging data can be overcome through carefully chosen assumptions and well-designed tagging studies (Brenden et al., 2010; Goethel et al., 2015, 2019; Saunders et al., 2019; Vincent et al., 2017, 2020). Therefore, in many instances, the benefits of including tagging data often outweigh the pitfalls for spatial IPMs (Goethel et al., 2019; Vincent et al., 2017, 2020). When only limited tag releases are possible, precision of spatial IPMs will likely decrease, but accuracy is not usually impacted (assuming that the dynamics of the tagged individuals, including movement, adequately reflect the overall population; Goethel et al., 2015b, 2019; Vincent et al., 2017). Additionally, many of the tag parameters (e.g. tag mixing and tag reporting rates) are estimable within IPMs (Figures S14–S15; Goethel et al., 2019; Vincent et al., 2017, 2020), particularly if auxiliary data are available and fit directly in the model (e.g. adding an objective function component for high reward tagging data as in Polacheck, Eveson, Laslett, Pollock, & Hearn, 2006). However, further work is needed to determine the optimal parametrization of reporting rates to adequately account for spatiotemporal variation in wide-ranging species harvested by diverse fleets, because direct

estimation can potentially add 10s to 100s of additional parameters (as is the case with Pacific tunas; Vincent, Pilling, & Hampton, 2019). Other parameters (e.g. tag loss and tag mortality) require direct inputs based on auxiliary experiments (e.g. double tagging or mortality studies) to avoid biased estimation in the IPM, but this information is routinely collected during tagging programs (Brenden et al., 2010; Cadigan & Bratney, 2006). With alternate tag types (e.g. electronic, genetic or natural), some of the issues associated with conventional tagging (e.g. tag reporting) may no longer apply, but new issues often arise (e.g. limited sample sizes due to cost limitations; Bravington, Skaug, & Anderson, 2016; Sippel et al., 2015). Ultimately, when spatial tag-integrated IPMs are being considered, clear communication is required between stock assessment analysts and scientists developing tagging experiments. Open dialogue among scientists will help ensure that tagging experimental designs address estimation of any potential tagging “nuisance” parameters, even though these issues are often thoroughly addressed in most tagging programs (Brenden et al., 2010; Goethel et al., 2015b; Vincent et al., 2020). In many instances, though, spatially stratified IPMs can still be implemented without incorporating tagging data (Punt, 2019a, 2019b). For instance, the *NO_TAG* IPM demonstrated adequate performance for many of the movement scenarios (except the climate-induced movement OM), corroborating the conclusions of Hulson et al., (2011), Hulson et al., (2013), McGilliard et al. (2015), Goethel et al. (2019) and Punt (2019a) that spatial IPMs are often feasible without incorporating tagging data.

Ultimately, the utility and need for spatial population models is context dependent and varies based on the biology of the species, the data available, the dynamics of harvesters and the robustness of the management framework (Berger et al., 2017; Cadrin, Goethel, Morse, Gay, & Kerr, 2019). Correctly identifying spatial population components (i.e., through population identification methods) and aligning biological, modelling and management units are often a prerequisite for developing robust conservation measures (Cadrin, 2020). In addition to representing best ecological practices, aligning the scale of modelled population units with observed biological structure may also be sufficient for developing robust harvest strategies for some species without the need for estimating movement (Bosley et al., 2019; Goethel et al., 2015a, 2015b; Kerr et al., 2017). However, our analyses suggest that these situations are likely to be limited (e.g. to sessile species) and that strong age-based movement patterns will lead to highly biased estimates from IPMs that assume closed populations. Additionally, understanding and accounting for movement dynamics can be beneficial for developing more flexible spatial harvest approaches (Bosley et al., 2019; Goethel & Berger, 2017) and can improve understanding of how recruitment dynamics vary across space (i.e., determining reproductive resilience of a species; Lowerre-Barbieri et al., 2017). The use of tailored operating models conditioned on the observed and assumed dynamics of a given case study is needed to explore whether spatially stratified IPMs are necessary to adequately assess a given species or population (Cadrin, 2020; Goethel, Kerr, & Cadrin, 2016). Increased application of spatially explicit management strategy evaluations can

help identify the model complexity required to achieve sustainable management advice (e.g. Punt et al., 2017).

Generalized simulation approaches that incorporate generic, common biological and harvesting dynamics are useful tools for making theoretical advances in ecological understanding and developing best practices (Cadrin, 2020). Our generalized simulations were meant to emulate the common dynamics of a marine species with moderate longevity to provide basic guidance on parametrizing movement for spatially stratified IPMs. However, our results were based on a best-case scenario of spatial structure (i.e., assessment and biological units matched with no misspecification of population boundaries or biology) and model process error was only explored for the parametrization of movement. Although general conclusions held across simulated life-history types (e.g. short-lived versus long-lived), performance may degrade with additional misspecification, process error (e.g. in natural mortality or productivity) or biological complexity (e.g. an increased number of populations). In any real-world application of an IPM (regardless of assumed spatial structure and dynamics), fixed values of steepness or natural mortality are likely to lead to additional bias compared to our results, while estimation of these parameters is notoriously difficult (Conn et al., 2010; Lee, Maunder, Piner, & Methot, 2012; Vincent et al., 2017). Because spatial IPMs can interpret fluctuations in population abundance as either movement of fish, variation in productivity or shifts in mortality (Cadrin et al., 2019; Goethel et al., 2015b), bias in either steepness or natural mortality parameters may magnify estimation issues in spatial IPMs. Incorporating tagging data can help improve estimates of natural mortality in certain applications, because the tag-recapture observations provide further information on spatiotemporal variations in mortality (Goethel et al., 2019; Vincent et al., 2017). In most cases, natural mortality is likely to vary with age, but only limited research has explored the potential to estimate age-varying natural mortality in IPMs (e.g. Deroba & Schueller, 2013). The potential impacts on estimation when age variation in both movement and natural mortality occurs remain uncharacterized. Similarly, steepness estimation remains problematic, especially when productivity is relatively high (Conn et al., 2010; Lee et al., 2012), and estimation is likely to be further impeded within spatial models due to the difficulty in differentiating signals in productivity among populations (Vincent et al., 2017). Developing steepness priors based on life-history models (e.g. Thorson, 2020) is a promising and active area of stock assessment research, but further work is needed to understand the impact of misdiagnosing the spatial distribution of productivity.

Although our results underrepresent the bias that might be expected in a spatial IPM, we expect that the relative results (e.g. the min-max solution) would not be greatly impacted by incorporating further process error (e.g. incorrect steepness or natural mortality assumptions), because these would likely impact both the spatial and closed population IPMs similarly. Additionally, further improvements to our IPM framework could potentially enhance the performance of spatially stratified IPMs. For instance, treating time-varying recruitment deviations and movement rates as

random effects would help reduce the number of effective parameters that need to be estimated (Maunder, Skaug, Fournier, & Hoyle, 2009; Thorson, Hicks, & Methot, 2015; Thorson & Minto, 2015). Treating recruitment and movement as random effects may also help reduce the inherent correlation between these parameters when treated as fixed effects and is likely to lead to improved performance of the full time and age-varying movement (YR+AG) IPM.

Spatially explicit IPMs often require increased assumptions and are viewed as more data intensive compared to spatially aggregated assessment models (Punt, 2019a, 2019b). Yet, they are better able to maximize the information content of data, while forcing explicit decisions regarding many assumptions that are implicit within spatially aggregated approaches (Berger et al., 2017). But, unique challenges for implementing spatially stratified or spatiotemporal IPMs remain. Spatially stratified models have scale dependency tradeoffs where precision may decrease as the number of modelled spatial units increases (i.e., due to reduced sample sizes and an increasing number of estimated parameters; Cao et al., 2020; Cope & Punt, 2011; Punt, 2019b). The current study assumed limited biological complexity by modelling only two populations, but other simulations studies have proven that spatial IPMs can be adequately applied with both an increased number of populations (e.g. upwards of ten subpopulations; Punt et al., 2018) and more complex population structures (e.g. natal homing; Vincent et al., 2017, 2020). However, robustness is likely dependent on accurate determination of population units and misalignment between true population boundaries and those assumed within the spatial assessment model may degrade IPM performance (Berger et al. In Review). As noted, spatial models matched to the scales of population identification information, including observed heterogeneity in demographics, productivity or harvest, will likely provide the best possible performance by ensuring that assessment and management population boundaries match the available data on population structure. Ultimately, the "optimal" number of populations or areas to include in a spatially stratified IPM will be context dependent. Based on spatially explicit simulations of small pelagic fish, Punt et al. (2018) demonstrated that it is often better to err on the side of modelling too many populations than too few, as long as there is evidence for spatial heterogeneity in population demographics or productivity, but the sample size versus precision trade-off should be carefully considered. Additionally, complex movement patterns have often been considered too difficult to estimate (Goethel et al., 2011, 2015b), but our results demonstrate that movement estimation may not be as problematic as previously envisioned.

Unlike spatially stratified IPMs, the assumption of a spatially continuous domain utilized in spatiotemporal models can better account for the continuum of spatial structure observed in many species that do not exhibit truly discrete population units. However, spatiotemporal models rely on fine-scale data collection, particularly from fishery-independent surveys of abundance (Cao et al., 2020), which are not available for many species and

may be recorded at very coarse spatiotemporal scales for historical data (Berger et al., 2017). Spatiotemporal models may also have trouble interpreting fine-scale spatial variability in fishery catch rate data (Mormede, Parker, & Pinkerton, 2020). Despite the limitations, spatially explicit IPMs are powerful tools that are able to better account for the observed spatial variability of harvested populations compared to spatially aggregated models that ignore fine-scale population dynamics (Berger et al., 2017). We envision that application of both spatiotemporal and spatially stratified modelling approaches will lead to co-evolution of methods for modelling spatial population processes (e.g. incorporating spatial autocorrelation approaches from spatiotemporal models into spatially stratified IPMs). Increased implementation of cross-model simulation testing (e.g. using spatiotemporal OMs and applying spatially stratified IPMs) may further elucidate spatially explicit IPM performance, while general robustness testing of spatial IPMs could be improved by utilizing agent-based OMs that demonstrate emergent population properties based on individual-level mechanistic dynamics of both the resource and harvesters.

Ultimately, the primary benefit of spatial IPMs (irrespective of underlying model structure) is the ability to incorporate disparate data types that span various spatiotemporal scales, which can then be fit within a unified estimation framework that allows modelling population dynamics across a species' range (Regehr et al., 2018; Saunders et al., 2019). Data are thus fit closer to the spatial scale of collection, which helps overcome sample size limitations across the spatial domain (Cao et al., 2020; Goethel et al., 2011). Additionally, integrated models are amenable to incorporation of a variety of auxiliary data sources (e.g. tagging data), which often enhances the performance of spatial IPMs (Figure S11; Goethel et al., 2019; Maunder & Punt, 2013). However, an array of alternative spatially explicit data sources exist that are often underutilized, even though they could help inform distributional shifts, levels of movement among population units and variability in mortality across the species range. For instance, genetics (e.g. population composition, close-kin mark-recapture and environmental DNA; Bravington et al., 2016; Yamamoto et al., 2016), drone surveys and satellite imaging (Lowerre-Barbieri et al., 2019), and vessel monitoring systems (i.e., to track fishing vessel harvest locations; Gerritsen & Lordan, 2011) can all be incorporated into IPMs. Similarly, citizen-science data and stakeholder traditional environmental knowledge (TEK) can be utilized to inform priors or parametrize models (Lopes, Verba, Begossi, & Pennino, 2019; Sun, Royle, & Fuller, 2019). Spatially explicit IPMs can also account for scale dependencies in population dynamics (Goethel et al., 2011; Plard et al., 2019). For instance, biophysical individual-based models, which account for larval drift via fine-scale ocean circulation models, can be imbedded directly in an IPM (e.g. Archambault et al., 2016) to better address the spatial dynamics of early life-history stages. As technology continues to evolve and bio-logging data become more widespread, IPMs must adapt to better utilize these unique data sources, which should lead to improved feasibility of implementing spatially explicit IPMs.

5 | CONCLUSIONS

Accounting for the impacts of climate change on species productivity and movement represents a major challenge for population models. Our results indicate that spatially stratified IPMs are able to estimate age- and time-varying connectivity due to climate-induced and ontogenetic movement even with little a priori knowledge regarding mixing levels or connectivity pathways. However, the biological complexity assumed in our simulation study was greatly simplified compared to observed dynamics for many marine fish populations and we incorporated only limited process error. Yet, based on our results and those of previous simulations with spatial IPMs, it is expected that, in most instances where spatial dynamics are present, spatially explicit IPMs are likely to outperform spatially aggregated counterparts. Caution is advised, though, when attempting to generalize these results to a real-world case study without first developing tailored operating models and associated simulations (Goethel et al., 2016). Application of spatial IPMs requires careful model development and validation to better understand the critical population processes influencing a given system, as well as the interactions among population units (Kerr & Goethel, 2014). Additionally, as environmental conditions continue to rapidly transform due to climate impacts, implementing spatially stratified models that can adequately account for changing species distributions will likely require incorporation of alternative data sources to help estimate the magnitude and direction of redistribution. A variety of spatially explicit data sets exist for marine species and the onus now lies with population modellers to determine approaches to better incorporate available spatial data into IPMs (Crossin et al., 2017; Lowerre-Barbieri et al., 2019; Plard et al., 2019). It is unlikely that any single spatial modelling approach will be able to address the array of spatial dynamics observed in animal populations, while also being able to incorporate the increasing number of fine-scale data sets being collected (Berger et al., 2017; Cadrin, 2020; Mormede et al., 2020). Cross-framework spatial applications will likely be required to maximize the information content of observed data, while incorporating the multiscalar spatial processes detected in real-world populations (Berger et al., 2017). We envision that co-development and integration of spatiotemporal and spatially stratified approaches may help overcome the limitations of either approach applied independently, as well as the limitations associated with simply ignoring spatial structure (as is typically done in IPMs of marine resources), and will lead to important advances in spatial ecology.

ACKNOWLEDGEMENTS

The scientific results and conclusions, as well as any views or opinions expressed herein, are those of the authors and do not necessarily reflect those of NOAA or the Department of Commerce. Funding was provided through a NOAA Stock Assessment Analytical Methods (SAAM) grant. We thank Michelle Masi, André Punt and three anonymous reviewers for improving earlier versions of the manuscript.

DATA AVAILABILITY STATEMENT

Data sharing is not applicable to this article as no new data were created or analysed in this study.

ORCID

Daniel R. Goethel  <https://orcid.org/0000-0003-0066-431X>

REFERENCES

- Allen, A. M., & Singh, N. J. (2016). Linking Movement Ecology with Wildlife Management and Conservation. *Frontiers in Ecology and Evolution*, 3, 155. <https://doi.org/10.3389/fevo.2015.00155>
- Archambault, B., Le Pape, O., Baulier, L., Vermard, Y., Veron, M., & Rivot, E. (2016). Adult-mediated connectivity affects inferences on population dynamics and stock assessment of nursery-dependent fish populations. *Fisheries Research*, 181, 198–213. <https://doi.org/10.1016/j.fishres.2016.03.023>
- Badjeck, M.-C., Allison, E. H., Halls, A. S., & Dulvy, N. K. (2010). Impacts of climate variability on fishery-based livelihoods. *Marine Policy*, 34, 375–383. <https://doi.org/10.1016/j.marpol.2009.08.007>
- Barbeaux, S. J., & Hollowed, A. B. (2018). Ontogeny matters: Climate variability and effects on fish distribution in the eastern Bering Sea. *Fisheries Oceanography*, 27, 1–15. <https://doi.org/10.1111/fog.12229>
- Berger, A. M., Deroba, J. J., Bosley, K. M., Goethel, D. R., Langseth, B. J., Schueller, A. M., and Hanselman, D. H. (In Review). Incoherent dimensionality in fisheries management: Consequences of misaligned stock assessment and population boundaries. *ICES Journal of Marine Science*.
- Berger, A. M., Goethel, D. R., Lynch, P. D., Quinn, T. II, Mormede, S., McKenzie, J., & Dunn, A. (2017). Space oddity: The mission for spatial integration. *Canadian Journal of Fisheries and Aquatic Sciences*, 74, 1698–1716. <https://doi.org/10.1139/cjfas-2017-0150>
- Beverton, R. J. H., & Holt, S. J. (1957). *On the dynamics of exploited fish populations*. London: Chapman and Hall.
- Bocedi, G., Pe'er, G., Heikkinen, R. K., Matsinos, Y., & Travis, J. M. J. (2012). Projecting species' range expansion dynamics: Sources of systematic biases when scaling up patterns and processes. *Methods in Ecology and Evolution*, 3, 1008–1018. <https://doi.org/10.1111/j.2041-210X.2012.00235.x>
- Bosley, K. M., Goethel, D. R., Berger, A. M., Deroba, J. J., Fenske, K. H., Hanselman, D. H., ... Schueller, A. M. (2019). Overcoming challenges of harvest quota allocation in spatially structured populations. *Fisheries Research*, 220, <https://doi.org/10.1016/j.fishres.2019.105344>
- Bravington, M. V., Skaug, H. J., & Anderson, E. C. (2016). Close-kin mark-recapture. *Statistical Science*, 31, 259–274. <https://doi.org/10.1214/16-STS552>
- Brenden, T. O., Jones, M. L., & Ebener, M. P. (2010). Sensitivity of tag-recovery mortality estimates to inaccuracies in tag shedding, handling mortality, and tag reporting. *Journal of Great Lakes Research*, 36, 100–109. <https://doi.org/10.1016/j.jglr.2009.09.002>
- Brownie, C., Hines, J. E., Nichols, J. D., Pollock, K. H., & Hestbeck, J. B. (1993). Capture-recapture studies for multiple strata including non-Markovian transition probabilities. *Biometrics*, 49, 1173–1187. <https://doi.org/10.2307/2532259>
- Cadigan, N. G., & Bratley, J. (2006). Reporting and shedding rate estimates from tag-recovery experiments on Atlantic cod (*Gadus morhua*) in coastal Newfoundland. *Canadian Journal of Fisheries and Aquatic Sciences*, 63, 1944–1958. <https://doi.org/10.1139/f06-096>
- Cadrin, S. X. (2020). Defining spatial structure for fishery stock assessment. *Fisheries Research*, 221, <https://doi.org/10.1016/j.fishres.2019.105397>
- Cadrin, S. X., Goethel, D. R., Morse, M. R., Gay, F., & Kerr, L. A. (2019). "So, where do you come from?" The impact of assumed spatial

- population structure on estimates of recruitment. *Fisheries Research*, 217, 156–168. <https://doi.org/10.1016/j.fishres.2018.11.030>
- Cao, J., Thorson, J. T., Punt, A., & Szuwalski, C. (2020). A novel spatio-temporal stock assessment framework to better address fine-scale species distributions: Development and simulation testing. *Fish and Fisheries*, 21, 350–367. <https://doi.org/10.1111/faf.12433>
- Carruthers, T. R., Walter, J. F., McAllister, M. K., & Bryan, M. D. (2015). Modeling age-dependent movement: An application to red and gag groupers in the Gulf of Mexico. *Canadian Journal of Fisheries and Aquatic Sciences*, 72, 1159–1176. <https://doi.org/10.1139/cjfas-2014-0471>
- Chandler, R. B., & Clark, J. D. (2014). Spatially explicit integrated population models. *Methods in Ecology and Evolution*, 5, 1351–1360. <https://doi.org/10.1111/2041-210X.12153>
- Ciannelli, L., Fisher, J. A. D., Skern-Mauritzen, M., Hunsicker, M. E., Hidalgo, M., Frank, K. T., & Bailey, K. M. (2013). Theory, consequences and evidence of eroding population structure in harvested marine fishes: A review. *Marine Ecology Progress Series*, 480, 227–243. <https://doi.org/10.3354/meps10067>
- Conn, P. B., Williams, E. H., & Shertzer, K. W. (2010). When can we reliably estimate the productivity of fish stocks? *Canadian Journal of Fisheries and Aquatic Sciences*, 67, 511–523. <https://doi.org/10.1139/F09-194>
- Cope, J. M., & Punt, A. E. (2011). Reconciling stock assessment and management scales under conditions of spatially varying catch histories. *Fisheries Research*, 107, 22–38. <https://doi.org/10.1016/j.fishres.2010.10.002>
- Crossin, G. T., Heupel, M. R., Holbrooke, C. M., Hussey, N. E., Lowerre-Barbieri, S. K., Nguyen, V. M., ... Cooke, S. J. (2017). Acoustic telemetry and fisheries management. *Ecological Applications*, 27, 1031–1049. <https://doi.org/10.1002/eap.1533>
- Deroba, J. J., & Schueller, A. M. (2013). Performance of stock assessments with misspecified age- and time-varying natural mortality. *Fisheries Research*, 146, 27–40. <https://doi.org/10.1016/j.fishres.2013.03.015>
- Fournier, D. A., Skaug, H. J., Ancheta, J., Ianelli, J., Magnusson, A., Maunder, M. N., ... Sibert, J. (2012). AD Model Builder: Using automatic differentiation for statistical inference of highly parameterized complex nonlinear models. *Optimization Methods and Software*, 27, 233–249. <https://doi.org/10.1080/10556788.2011.597854>
- Fu, C., & Fanning, L. P. (2004). Spatial considerations in the management of Atlantic cod off Nova Scotia, Canada. *North American Journal of Fisheries Management*, 24, 775–784. <https://doi.org/10.1577/M03-134.1>
- Gerritsen, H., & Lordan, C. (2011). Integrating vessel monitoring system (VMS) data with daily catch data from logbooks to explore the spatial distribution of catch and effort at high resolution. *ICES Journal of Marine Science*, 68, 245–252. <https://doi.org/10.1093/icesjms/fsq137>
- Goethel, D. R., & Berger, A. M. (2017). Accounting for spatial complexities in the calculation of biological reference points: Effects of misdiagnosing population structure for stock status indicators. *Canadian Journal of Fisheries and Aquatic Sciences*, 74, 1878–1894. <https://doi.org/10.1139/cjfas-2016-0290>
- Goethel, D. R., Bosley, K. M., Hanselman, D. H., Berger, A. M., Deroba, J. J., Langseth, B. J., & Schueller, A. M. (2019). Exploring the utility of different tag-recovery experimental designs for use in spatially explicit, tag-integrated stock assessment models. *Fisheries Research*, 219, 105320. <https://doi.org/10.1016/j.fishres.2019.105320>
- Goethel, D., Kerr, L. A., & Cadrin, S. X. (2016). Incorporating spatial population structure into the assessment-management interface of marine resources. In C. T. T. Edwards, & D. J. Dankel (Eds.), *Management Science in Fisheries: An introduction to Simulation-Based Methods* (pp. 319–347). London: Taylor & Francis.
- Goethel, D. R., Legault, C. M., & Cadrin, S. X. (2015a). Demonstration of a spatially explicit, tag-integrated stock assessment model with application to three interconnected stocks of yellowtail flounder off of New England. *ICES Journal of Marine Science*, 72, 582–601. <https://doi.org/10.1093/icesjms/fsu014>
- Goethel, D. R., Legault, C. M., & Cadrin, S. X. (2015b). Testing the performance of a spatially explicit tag-integrated stock assessment model of yellowtail flounder (*Limanda ferruginea*) through simulation analysis. *Canadian Journal of Fisheries and Aquatic Sciences*, 72, 164–177. <https://doi.org/10.1139/cjfas-2014-0244>
- Goethel, D. R., Quinn, T. J. II, & Cadrin, S. X. (2011). Incorporating spatial structure in stock assessment: Movement modelling in marine fish population dynamics. *Reviews in Fisheries Science and Aquaculture*, 19, 119–136. <https://doi.org/10.1080/10641262.2011.557451>
- Hidalgo, M., Secor, D. H., & Browman, H. I. (2016). Observing and managing seascapes: Linking synoptic oceanography, ecological processes, and geospatial modelling. *ICES Journal of Marine Science*, 73, 1825–1830. <https://doi.org/10.1093/icesjms/fsw079>
- Hilborn, R., & Walters, C. J. (1992). *Quantitative Fisheries Stock Assessment: Choice, Dynamics, and Uncertainty*. New York: Chapman and Hall.
- Hughes, S., Yau, A., Max, L., Petrovic, N., Davenport, F., Marshall, M., ... Cinner, J. E. (2012). A framework to assess national level vulnerability from the perspective of food security: The case of coral reef fisheries. *Environmental Science and Policy*, 23, 95–108. <https://doi.org/10.1016/j.envsci.2012.07.012>
- Hulson, P.-J. F., Miller, S. E., Ianelli, J. N., & Quinn, T. J. II (2011). Including mark-recapture data into a spatial age-structured model: Walleye pollock (*Theragra chalcogramma*) in the eastern Bering Sea. *Canadian Journal of Fisheries and Aquatic Sciences*, 68, 1625–1634. <https://doi.org/10.1139/f2011-060>
- Hulson, P.-J. F., Quinn, T. J. II, Hanselman, D. H., & Ianelli, J. N. (2013). Spatial modelling of Bering Sea walleye Pollock with integrated age-structured assessment models in a changing environment. *Canadian Journal of Fisheries and Aquatic Sciences*, 70, 1–15. <https://doi.org/10.1139/cjfas-2013-0020>
- Hurtado-Ferro, F., Punt, A. E., & Hill, K. T. (2014). Use of multiple selectivity patterns as a proxy for spatial structure. *Fisheries Research*, 158, 102–115. <https://doi.org/10.1016/j.fishres.2013.10.001>
- Jeltsch, F., Bonte, D., Pe'er, G., Reineking, B., Leimgruber, P., Balkenhol, N., ... Bauer, S. (2013). Integrating movement ecology and biodiversity research – exploring new avenues to address spatiotemporal biodiversity dynamics. *Movement Ecology*, 1, 1–13. <https://doi.org/10.1186/2051-3933-1-6>
- Karp, M. A., Peterson, J. O., Lynch, P. D., Griffis, R. B., Adams, C. F., Arnold, W. S., ... Link, J. S. (2019). Accounting for shifting distributions and changing productivity in the development of scientific advice for fishery management. *ICES Journal of Marine Science*, 76, 1305–1315. <https://doi.org/10.1093/icesjms/fsz048>
- Kerr, L. A., & Goethel, D. R. (2014). Simulation modelling as a tool for synthesis of stock identification information. In S. X. Cadrin, L. A. Kerr, & S. Mariani (Eds.), *Stock Identification Methods: An Overview* (pp. 501–533). Burlington: Elsevier Science and Technology.
- Kerr, L. A., Hintzen, N. T., Cadrin, S. X., Clausen, L. W., Dickey-Collas, M., Goethel, D. R., ... Nash, R. D. M. (2017). Lessons learned from practical approaches to reconcile mismatches between biological population structure and stock units of marine fish. *ICES Journal of Marine Science*, 74, 1708–1722. <https://doi.org/10.1093/icesjms/fsw188>
- Lee, H.-H., Maunder, M. N., Piner, K. R., & Methot, R. D. (2012). Can steepness of the stock-recruitment relationship be estimated in fishery stock assessment models? *Fisheries Research*, 125–126, 254–261. <https://doi.org/10.1016/j.fishres.2012.03.001>
- Lee, H.-H., Piner, K., Maunder, M., Taylor, I., & Methot, R. (2017). Evaluation of alternative modelling approaches to account for spatial effects due to age-based movement. *Canadian Journal of Fisheries and Aquatic Sciences*, 74, 1832–1844. <https://doi.org/10.1139/cjfas-2016-0294>

- Link, J. S., Nye, J. A., & Hare, J. A. (2011). Guidelines for incorporating fish distribution shifts into a fisheries management context. *Fish and Fisheries*, 12, 461–469. <https://doi.org/10.1111/j.1467-2979.2010.00398.x>
- Lopes, P. F. M., Verba, J. T., Begossi, A., & Pennino, M. G. (2019). Predicting species distribution from fishers' local ecological knowledge: A new alternative for data-poor management. *Canadian Journal of Fisheries and Aquatic Sciences*, 76, 1423–1431. <https://doi.org/10.1139/cjfas-2018-0148>
- Lowerre-Barbieri, S. K., DeCelles, G., Pepin, P., Catalan, I. A., Muhling, B., Erisman, B., ... Paris, C. B. (2017). Reproductive resilience: A paradigm shift in understanding spawner-recruit systems in exploited marine fish. *Fish and Fisheries*, 18, 285–312. <https://doi.org/10.1111/faf.12180>
- Lowerre-Barbieri, S. K., Kays, R., Thorson, J. T., & Wikelski, M. (2019). The ocean's movescape: Fisheries management in the bio-logging decade (2018–2028). *ICES Journal of Marine Science*, 76, 477–488. <https://doi.org/10.1093/icesjms/fsy211>
- Maunder, M. N., & Punt, A. E. (2013). A review of integrated analysis in fisheries stock assessment. *Fisheries Research*, 142, 61–74. <https://doi.org/10.1016/j.fishres.2012.07.025>
- Maunder, M. N., Skaug, H. J., Fournier, D. A., & Hoyle, S. D. (2009). Comparison of Fixed Effect, Random Effect, and Hierarchical Bayes Estimators for Mark Recapture Data Using AD Model Builder. In D. L. Thompson, E. G. Cooch, & M. J. Conroy (Eds.), *Modeling Demographic Processes in Marked Populations* (pp. 917–946). Boston: Springer.
- McGilliard, C. R., Punt, A. E., Methot, R. D., & Hilborn, R. (2015). Accounting for marine reserves using spatial stock assessments. *Canadian Journal of Fisheries and Aquatic Sciences*, 72, 262–280. <https://doi.org/10.1139/cjfas-2013-0364>
- Mormede, S., Parker, S. J., & Pinkerton, M. H. (2020). Comparing spatial distribution modelling of fisheries data with single-area or spatially-explicit integrated population models, a case study of toothfish in the Ross Sea region. *Fisheries Research*, 221, <https://doi.org/10.1016/j.fishres.2019.105381>
- Murphy, J. T. (2020). Climate change, interspecific competition, and poleward vs. depth distribution shifts: Spatial analyses of the eastern Bering Sea snow and Tanner crab (*Chionoecetes opilio* and *C. bairdi*). *Fisheries Research*, 223, <https://doi.org/10.1016/j.fishres.2019.105417>
- Nathan, R., Getz, W. M., Revilla, E., Holyoak, M., Kadmon, R., Saltz, D., & Smouse, P. E. (2008). A movement ecology paradigm for unifying organismal movement research. *PNAS*, 105, 19052–19059. <https://doi.org/10.1073/pnas.0800375105>
- Pecl, G. T., Araujo, M. B., Bell, J. D., Blanchard, J., Bonebrake, T. C., Chen, I.-C., ... Williams, S. E. (2017). Biodiversity redistribution under climate change: Impacts on ecosystems and human well-being. *Science*, 355, <https://doi.org/10.1126/science.aai9214>
- Plard, F., Fay, R., Kery, M., Cohas, A., & Schaub, M. (2019). Integrated population models: Powerful methods to embed individual processes in population dynamics models. *Ecology*, 100, e02715. <https://doi.org/10.1002/ecy.2715>
- Polacheck, T., Eveson, J. P., Laslett, G. M., Pollock, K. H., & Hearn, W. S. (2006). Integrating catch-at-age and multiyear tagging data: A combined Brownie and Petersen estimation approach in a fishery context. *Canadian Journal of Fisheries and Aquatic Sciences*, 63, 534–548. <https://doi.org/10.1139/f05-232>
- Punt, A. E. (2019a). Modelling recruitment in a spatial context: A review of current approaches, simulation evaluation of options, and suggestions for best practices. *Fisheries Research*, 217, 140–155. <https://doi.org/10.1016/j.fishres.2017.08.021>
- Punt, A. E. (2019b). Spatial stock assessment methods: A viewpoint on current issues and assumptions. *Fisheries Research*, 213, 132–143. <https://doi.org/10.1016/j.fishres.2019.01.014>
- Punt, A. E., Haddon, M., Little, L. R., & Tuck, G. N. (2016). Can a spatially-structured stock assessment address uncertainty due to closed areas? A case study based on pink ling in Australia. *Fisheries Research*, 175, 10–23. <https://doi.org/10.1016/j.fishres.2015.11.008>
- Punt, A. E., Haddon, M., Little, L. R., & Tuck, G. N. (2017). The effect of marine closures on a feedback control management strategy used in a spatially aggregated stock assessment: A case study based on pink ling in Australia. *Canadian Journal of Fisheries and Aquatic Sciences*, 74, 1960–1973. <https://doi.org/10.1139/cjfas-2016-0017>
- Punt, A. E., Okamoto, D. K., MacCall, A. D., Shelton, A. O., Armitage, D. R., Cleary, J. S., ... Woodruff, J. (2018). When are estimates of spawning biomass for small pelagic fishes improved by taking spatial structure into account? *Fisheries Research*, 206, 65–78. <https://doi.org/10.1016/j.fishres.2018.04.017>
- Quinn, T. J. II, Deriso, R. B., & Neal, P. R. (1990). Migratory catch age analysis. *Canadian Journal of Fisheries and Aquatic Sciences*, 47, 2315–2327. <https://doi.org/10.1139/f90-258>
- Regehr, E. V., Hostetter, N. J., Wilson, R. R., Rode, K. D., St. Martin, M., & Converse, S. J. (2018). Integrated population modeling provides the first empirical estimates of vital rates for polar bears in the Chukchi Sea. *Scientific Reports*, 8, 16780. <https://doi.org/10.1038/s41598-018-34824-7>
- Riecke, T. V., Williams, P. J., Behnke, T. L., Gibson, D., Leach, A. G., Sedinger, B. S., ... Sedinger, J. S. (2019). Integrated population models: Model assumptions and inference. *Methods in Ecology and Evolution*, 10, 1072–1082. <https://doi.org/10.1111/2041-210X.13195>
- Saunders, S. P., Farr, M. T., Wright, A. D., Bahlai, C., Ribeiro, J. W. Jr, Rossman, S., ... Zipkin, E. F. (2019). Disentangling data discrepancies with integrated population models. *Ecology*, 100, e02714. <https://doi.org/10.1002/ecy.2714>
- Sippel, T., Evenson, J. P., Galuardi, B., Lam, C., Hoyle, S., Maunder, M. N., ... Nicol, S. (2015). Using movement data from electronic tags in fisheries stock assessment: A review of models, technology, and experimental design. *Fisheries Research*, 163, 152–160. <https://doi.org/10.1016/j.fishres.2014.04.006>
- Sun, C. C., Royle, J. A., & Fuller, A. K. (2019). Incorporating citizen science in spatially explicit integrated population models. *Ecology*, 100, e02777. <https://doi.org/10.1002/ecy.2777>
- Thorson, J. T. (2020). Predicting recruitment density dependence and intrinsic growth rate for all fishes worldwide using a data-integrated life-history model. *Fish and Fisheries*, 21, 237–251. <https://doi.org/10.1111/faf.12427>
- Thorson, J. T., Hicks, A. C., & Methot, R. D. (2015). Random effect estimation of time-varying factors in Stock Synthesis. *ICES Journal of Marine Science*, 72, 178–185. <https://doi.org/10.1093/icesjms/fst211>
- Thorson, J. T., Jannot, J., & Somers, K. (2017). Using spatio-temporal models of population growth and movement to monitor overlaps between human impacts and fish populations. *Journal of Applied Ecology*, 54, 577–587. <https://doi.org/10.1111/1365-2664.12664>
- Thorson, J. T., & Minto, C. (2015). Mixed effects: A unifying framework for statistical modelling in fisheries biology. *ICES Journal of Marine Science*, 72, 1245–1256. <https://doi.org/10.1093/icesjms/fsu213>
- Vincent, M. T., Brenden, T. O., & Bence, J. R. (2017). Simulation testing the robustness of a multi-region tag-integrated assessment model that exhibits natal homing and estimates natural mortality and reporting rate. *Canadian Journal of Fisheries and Aquatic Sciences*, 74, 1930–1949. <https://doi.org/10.1139/cjfas-2016-0297>
- Vincent, M. T., Brenden, T. O., & Bence, J. R. (2020). Parameter estimation performance of a recapture-conditioned integrated catch-at-age analysis model. *Fisheries Research*, 224, <https://doi.org/10.1016/j.fishres.2019.105451>
- Vincent, M. T., Pilling, G. M., & Hampton, J. (2019). *Stock assessment of skipjack tuna in the western and central Pacific Ocean* (SPC Publication No. WCPFC-SC15-2019/SA-WP-05-Rev2). Western and Central Pacific Fisheries Commission, Oceanic Fisheries Program, The Pacific Community. Available from <https://www.wcpfc.int/system/files/SC15-SA-WP-05%20SKJ-Assessment%20REV2.pdf>

- White, J. W. (2015). Marine reserve design theory for species with ontogenetic migration. *Biology Letters*, *11*, 20140511. <https://doi.org/10.1098/rsbl.2014.0511>.
- Yamamoto, S., Minami, K., Fukaya, K., Takahashi, K., Sawada, H., Murakami, H., ... Kondoh, M. (2016). Environmental DNA as a 'snapshot' of fish distribution: A case study of Japanese jack mackerel in Maizuru Bay. *Sea of Japan. Plos ONE*, *11*, e0149786. <https://doi.org/10.1371/journal.pone.0149786>.
- Ying, Y., Chen, Y., Lin, L., & Gao, T. (2011). Risks of ignoring fish population spatial structure in fisheries management. *Canadian Journal of Fisheries and Aquatic Sciences*, *68*, 2101-2120. <https://doi.org/10.1139/f2011-116>.
- Zipkin, E. F., & Saunders, S. P. (2018). Synthesizing multiple data types for biological conservation using integrated population models. *Biological Conservation*, *217*, 240-250. <https://doi.org/10.1016/j.biocon.2017.10.017>.

SUPPORTING INFORMATION

Additional supporting information may be found online in the Supporting Information section.

How to cite this article: Goethel DR, Bosley KM, Langseth BJ, et al. Where do you think you're going? Accounting for ontogenetic and climate-induced movement in spatially stratified integrated population assessment models. *Fish Fish*. 2021;22:141-160. <https://doi.org/10.1111/faf.12510>